Master's Thesis

Characterization and Modeling of Thermoelectric Properties of Fiber-Reinforced and Multiscale Hybrid Composites

DAE HAN SUNG

Department of Mechanical Engineering

Graduate School of UNIST

2016

Characterization and Modeling of Thermoelectric Properties of Fiber-Reinforced and Multiscale Hybrid Composites

DAE HAN SUNG

Department of Mechanical Engineering

Graduate School of UNIST

Characterization and Modeling of Thermoelectric Properties of Fiber-Reinforced and Multiscale Hybrid Composites

A thesis
submitted to the Graduate School of UNIST
in partial fulfillment of the
requirements for the degree of
Master of Science

DAE HAN SUNG

6/1/2016

Approved by

Advisor
Young-Bin Park

Characterization and Modeling of Thermoelectric Properties of Fiber-Reinforced and Multiscale Hybrid Composites

DAE HAN SUNG

This certifies that the thesis of DAE HAN SUNG is approved.

6/1/2016

Advisor: Young-Bin Park

Hyung Wook Park

Han Gi Chae

Wooseok Ji

Myungsoo Kim

Abstract

Thermoelectricity is one of the energy harvesting techniques that converts waste heat into electrical energy by using a thermoelectric device, which has been confined to metal semiconducting materials. Although inorganic conductors and semiconductors can serve as efficient thermoelectric materials, they have such drawbacks as high processing costs, scarcity and toxicity. For these reasons, organic electronic materials have received attention, and research on thermoelectric systems has been conducted utilizing either conjugated polymers or carbon nanotubes (CNT)/polymer composites to date.

We have focused on composites consisting of reinforcing woven fibers as thermoelectric materials, in conjunction with functionalization of woven fabric composites, which can serve as structural materials. We have characterized the thermal and electrical conductivities and Seebeck coefficients of fiber-reinforced composites, which are the constituents of thermoelectric efficiency factor, and confirmed the feasibility of using composites for thermoelectrics. In addition, numerical modeling approaches were developed to predict the thermal and electrical conductivities of composites and to optimize the figure of merit, an index for thermoelectric efficiency, with respect to such material variables as fiber volume fraction, aspect ratio and orientation.

Two types of composites, namely, carbon nanotube (CNT)/glass fiber (GF)/epoxy multiscale hybrid composites and carbon fiber (CF)/epoxy composites, were fabricated, and their thermoelectric properties were evaluated as n-/p-type thermoelectric materials. Experimental results showed that the electrical resistivity of the CNT/GF/epoxy composites decreased as CNT concentration increased. In-plane samples showed higher electrical and thermal conductivities due to partial alignment of CNTs in the multiscale composites and continuity of CFs in CF/epoxy composites. In general, CF/epoxy composites showed better electrical and thermal conductivities than multiscale composites. In the Seebeck coefficient measurement test, the multiscale composites showed n-type thermoelectric behavior, whereas the CF/epoxy composites showed p-type behavior. When temperature gradients were applied to closed circuits comprised of multiscale composites and CF/epoxy composites as n- and p-type materials, respectively, an electric current was successfully generated.

In the process of optimizing the figure of merit, modeling approaches combining the methods for nanocomposites and woven fabric composites were proposed to predict the thermal and electrical conductivities of composites. The Mori-Tanaka method, thermal-electrical analogy and rule-of-mixtures were adopted as the modeling tools, and we validated the modeling approaches through comparison with experimental data. Thermal-electrical analogy and modified Mori-Tanaka method predictions, which take into account fiber volume fraction, conductivity, aspect ratio, continuity and undulation, agreed well with experimental results.

This study covers evaluation of the thermoelectric properties of composites in which reinforcing woven fibers are incorporated, including manufacturing and characterization of materials, structure of

constituting materials, and validity of the composites as thermoelectric materials. We proposed and validated the modeling methodologies to predict the thermal and electrical conductivities of composites, taking into account the influences of constituents' structure, geometry and properties.

The outcome of this study is expected to pave the way for a new method for energy harvesting where base materials are structural polymer composites that include reinforcing fibers and polymer matrix. Potential applications range from small devices like electronic and home appliances to large structures such as automotive, aerospace and civil structures. The uses of conductivity models developed can be expanded into other multifunctional applications, such as materials design for thermal management, electrostatic discharging, electromagnetic interference shielding, etc.

Contents

List of Figures

Figure 4-10 Electrical conductivity modeling and empirical data of CF/epoxy composites vs. CF volume fraction: (a) In-plane, (b) Through-thickness

List of Tables

1. Introduction

Fossil fuels, including petroleum, coal and natural gas, are used as the world's primary energy resource. Fossil fuels that are formed by the anaerobic decomposition of remains of dead organisms millions of years ago have facilitated the development of worldwide economy and have become the significant foundation of modern civilization since the industrial revolution. It is controversial whether the resources are going to be exhausted in a few decades or last for a longer period of time. Setting aside an argument, it is obvious that the fossil fuels are finite resources. A more critical problem on the resources is that they have been destroying the natural environment incorrigibly. According to the work of R. J. Andres et al.[1], greenhouse gases released to the atmosphere from the fossil fuel as a main contributor occupy 91% of the carbon dioxide concentration. These gases make the earth isolated from outside, which implies that drastic climate change occurs sometime. Shifting the excessive dependence on the traditional energy source to renewable and environment-friendly energy, it's expected that steep fuel consumption curve might have a gentle slope and catastrophic change might be postponed.

Among a variety of ways to make use of the renewable energy, thermoelectric technology has received attention enabling waste heat to be utilized by converting the heat energy to electrical energy. Heat flux and temperature gradient exist everywhere in the nature and the structures created by human beings, which offer us opportunities to harvest heat energy from the natural environment around us. A strong point of thermoelectric devices is that the slight amount of heat that traditional power generating system cannot take advantage of is able to generate electric current. The fact that they do not made a noise or vibration common in other generating system is another advantage since they are used by simple attachment or installation on a structure. Additionally, the energy converting devices perform not only a role of transforming heat into electric current but also the reverse process. This is explained by two mechanisms which compose thermoelectric theory.

Seebeck and Peltier effects were first observed to present in metals in 1820s and 30s, respectively. Seebeck effect indicates that if the junctions of two dissimilar materials are exposed to different temperatures at each end, voltage difference is developed which proportionate to the temperature gap. And Seebeck coefficient is defined by dividing the voltage difference by the applied temperature difference and is intrinsic property of the materials. Inversely, Peltier effect describes either absorbed or rejected heat at the junction when an electrical current passes through the junctions of two dissimilar materials. This effect is primarily because of the difference of Fermi energy level between the two adjacent materials.[2]

The discovery of thermoelectric materials in early stage was by means of a metal but continued profound studies have made semiconductors become main materials that have relatively high efficiency due to availability to control the Fermi level. Even though it is true that semiconductors, such as bismuth telluride, show state-of-the-art thermoelectric performance, it is not enough to commercialize and distribute them as products in low temperature range. It is figure of merit driven in order to compare

the efficiencies of individual materials in a view of thermoelectricity, considering intrinsic properties such as thermal and electrical conductance of the certain materials. Good thermoelectric materials are described by high Seebeck coefficient, high electrical conductivity and low thermal property. In general, a material with high electrical property tends to have good thermal conductivity and low Seebeck coefficient.

As conducting polymers are discovered, organic thermoelectric substances have been drawing attention with the fact that semiconducting materials have limitation in that they have considerable production costs, scarcity and toxicity. Organic polymers have such desirable aspect as thermal conductivity is very low to become a candidate for thermoelectric materials and a carbon, the basis element of polymers, is one of the most common and abundant elements on the face of the earth. Economical price, straightforward processibility, light weight and flexibility are also the factors that they attract public attention. Conjugated polymers such as polyacetylene (PA)[3,4], polypyrroles (PPy)[5] and polyanilines (PANI)[6] and modified nanocomposites[7] are the examples.

In this research, we have focused on the applicability of woven fabric composites mainly utilized as mechanical structural composites as thermoelectric materials and concentrated on the efficiency they possess. Thermoelectricity can be regarded as additional function like sensing ability, self-healing and electromagnetic interference shielding from the point of view of the fabric composites. It is anticipated that in automotive and aerospace industries the enhancement of usability of extra thermal energy created during the operation makes their systems managed more independently and effectively. We need to seek ways to maximize thermoelectric efficiency which means an optimization of figure of merit value.

First, we evaluated the thermoelectric properties of carbon nanotube (CNT)/glass fiber (GF)/epoxy multiscale composites and carbon fiber (CF)/epoxy fiber-reinforced composites by measuring the thermal, electrical conductivities and Seebeck coefficient. Figure of merit which is an intrinsic property of the final product varies with the variables of constituting materials, such as volume fraction, aspect ratio and geometry of the constituents. In order to fully understand the influences of the variables on the electrical and thermal conductivities composing figure of merit, conductivity modeling approached are proposed and evaluated.

2. Literature Review

2.1. Organic Thermoelectric Materials

In early stage of thermoelectricity, primary thermoelectric materials have been metals like bismuth telluride and many researchers focused on the static feature that are in the contrast with other dynamic devices such as motor or power generator. They have made an effort to elevate the efficiency that applied temperature gradient may be utilized as much as possible. Figure of merit, a dimensionless factor, is represented with the equation $ZT = (\alpha^2\sigma/\kappa)T$ where α, σ and κ denotes Seebeck coefficient, electrical conductivity and thermal conductivity, respectively. As can be inferred from the equation above, a material with good electrical property, Seebeck coefficient and poor thermal conductivity is a great candidate for thermoelectric materials. Increasing electrical conductivity or diminishing thermal conductivity improved ZT by means of modifying micro or nano structures of metal and inorganic materials, for instance, introduction of precipitates, rattlers and phase separation.[8-11] ZT is affected by ambient (service) temperature considerably since the factor is composed of the variables that are sensitive to the temperature. Common metal and inorganic thermoelectric materials are worthwhile to utilize as applications in high temperature condition but are not economical to operate them in low temperature range (< 200°C) because they demonstrate their effectiveness over 200°C. Additionally, they have negative aspects in terms of processibility, toxicity and scarcity though they are displaying the highest values of ZT.[12]

It is organic and polymer materials that are devised for the purpose of substituting metal and inorganic substances. Polymers hold a dominant position with respect to the massive production and supply due to such advantages as include non-toxicity, easy fabrication process, low material cost and scalability on the condition that the energy production efficiency is guaranteed. The invention of conducting polymers is a significant event which makes them prospective candidates for thermoelectric materials based on the fact that they act as insulator in terms of heat transfer. PA[3,4], PANI[6], PPy[5], PEDOT:PSS[13] are good examples. There are several ways in which the electrical conductivity of these conjugated polymers is improved. Electrochemical or chemical doping using oxidation-reduction reaction induces increase of main charge carriers just like electrons and holes which is followed by the enhancement of electrical property of the polymers. Though a little amount of doping concentration could be effective to promote the carriers' movement in the materials, the additional electrons make Fermi energy level shift upward passing by conduction band, thereby reducing Seebeck coefficient which is unfavorable to thermoelectric efficiency. Another factor is the mobility control of electrons by modifying molecular weight, polymer chain length, orientation and polymer concentration in mixture since the polymers are affected by the structure or mechanism of their chain.

One of the simplest ways to change the properties of a material is to make two substances into a compound whose nature is different from either of the two raw materials. Nanomaterials are primarily studied as mechanically reinforcing materials and nanocomposites obtain strengthening effect without

deteriorating the matrix by maximizing the influence of interphase. There are many ways in fabricating nanocomposites such as polymerization of the monomers, melt and solution blending. It's crucial to control the degree of nanomaterials' dispersion through overcoming the van der Waals force between them in the homogenization of heterogeneity and matrix. Researchers seek ways to achieve high Seebeck coefficient and electrical conductivity by blending semiconductor nanoparticles or carbon nanomaterials into the polymer matrix and those properties substantially vary with what materials they utilize. Along with the advantages, many studies have been conducted on how to offset the increased thermal conductivity of the composites due to the good thermal property of the heterogeneities.

CNT is the cylinder form of a rolled graphene sheet or multiple sheets which has hexagonal sp^2 hybridized carbon structure. CNT properties are significantly influenced by the arrangement of carbon atoms (chirality), exhibiting metallic or semiconducting characteristics relying on the chirality. For the sake of thermoelectricity, high electrical conductivity makes CNT suited for the purpose while good thermal property hinder it from being one of the efficient thermoelectric materials. L. Zhao et al. [14] employed aerogel method based on graphene and multi-walled CNTcomposites to increase Seebeck coefficient and electrical conductivity. They finally obtained the figure of merit value (ZT) of ~0.001, reducing thermal conductivity by means of three dimensional porous skeleton structure which scatters the movement of phonons. C. Meng et al.[15] proposed a new method to enhance thermoelectric properties by coating PANI around CNTs. They achieved markedly improved Seebeck coefficient and power factor from CNT/PANI composites, which cannot be gained by using either of the individual constituents. The research group described that they resulted from size-dependent energy-filtering effect. Fig. 2-1 represents the SEM images of a CNT sheet before and after PANI coating.

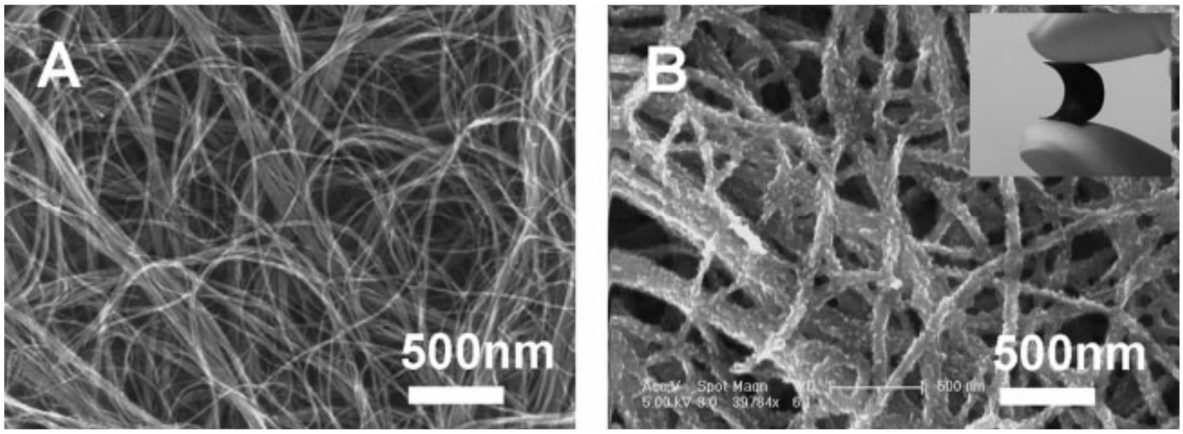

Fig. 2-1 SEM images of thick CNT sheet before and after PANI coating[15]

Fig. 2-2 shows the way of modifying thermoelectric properties at a glance suggested by C. Yu. et al.[16] They utilized aqueous polymer emulsions which created excluded space and pushed CNT fillers into outermost regions the polymers doesn't occupy. The segregated network formed by drying process made the composite electrically connected thereby the electrical conductivity was drastically enhanced

whereas the volume made by polymer emulsion causes the retention of thermal conductivity. The group concluded that figure of merit can be greatly improved by varying filler contents and concentration.

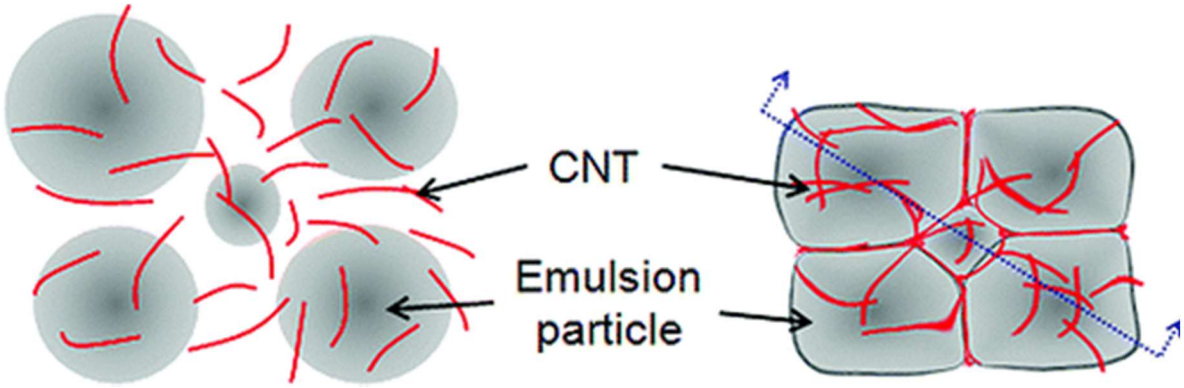

Fig. 2-2 Schematic of CNTs suspended in an aqueous emulsion and the emulsion-based composite after drying[16]

C.A. Hewitt et al.[17] created the multiple element modules by stacking MWCNT/polyvinylidene fluoride (PVDF) composite films. They demonstrated that linearly increasing thermoelectric voltage can be achieved by simple stacking of the films which is followed by enhanced power output. They expected that this fabric-modules will offer a realistic alternative to existing metal thermoelectric materials for light weight, flexible and portable devices. G.P. Moriarty et al.[18] reported that the use of stabilizer raised electrical property of the composite, remaining Seebeck coefficient and thermal conductivity. Intrinsically conductive polymer, poly(3,4-ethylenedioxythiophene) : poly(styrenesulfonate) (PEDOT:PSS), was taken as the stabilizer which assists SWNT network to be firmly developed, in turn, the thin film composites exhibit metallic electrical conductivity (~4.0e+5 S/m). Fig. 2-3 indicates the results from their experiments.

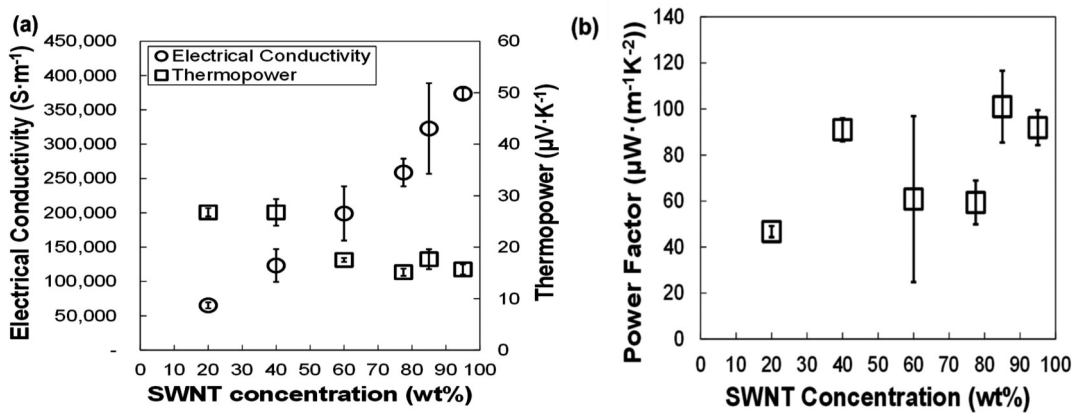

Fig. 2-3 Electrical conductivity, thermopower and power factor of SWNT/PEDOT:PSS films[18]

2.2. Multi-functionality of Composites

Fiber-reinforced composites are made up of fibers of eminent mechanical properties embedded in or attached to a matrix with distinct interfaces between them. Combining fibers and matrix leads to entirely new properties that cannot be achieved by individual components, retaining their physical and chemical identities. Fibers are generally the principal load-carrying constituent, while the matrix serves as a settling and load transfer medium and keep the fibers from damages such as chemicals and temperature.[19]

The traditional approach to develop structures is to address the load-carrying function and other functional requirements separately, resulting in a suboptimal load-bearing structure with add-on attachments which perform the non-structural functions with the penalty of added weight.[20] However, the concept of multi-functionality of material which describes the development of traditional load-carrying structural material incorporated with non-load-carrying functions without additional materials, for instance, actuation, electromagnetic interference shielding and self-healing.

Hybrid multiscale composites are also substantially attractive which consist of nanomaterials in the matrix as well as micro-scale fabric for the sake of mechanical property. In the works of Vlasveld et al.[21] and Zhao et al.[22], CNT is utilized to serve as a component reinforcing mechanical properties in transverse direction perpendicular continuous fiber by replacing polymer matrix with CNT-nanocomposites or growing CNT on the continuous fiber. Such adjunction of nanoparticles into the composites has offered tailorability and scalability with respect to a variety of manufacturing variables, thereby the diversity and profundity of multi-functionality have been guaranteed.

The most representative field where multi-functionality is applied is structural health monitoring (SHM) using piezoresistivity. A. Todoroki et al. proposed an electrical resistance change method with integrated probes attached on one side of the carbon fiber reinforced polymers (CFRP) composite structures' surface in order to detect the delamination and matrix cracking of the composites.[23,24] Fig. 2-4 describes the electrical resistance change method they employed. The group investigated the influence of many variables on the method empirically and numerically using finite element analysis (FEA) such as volume fraction of CF, electrode spacing distance, etc.

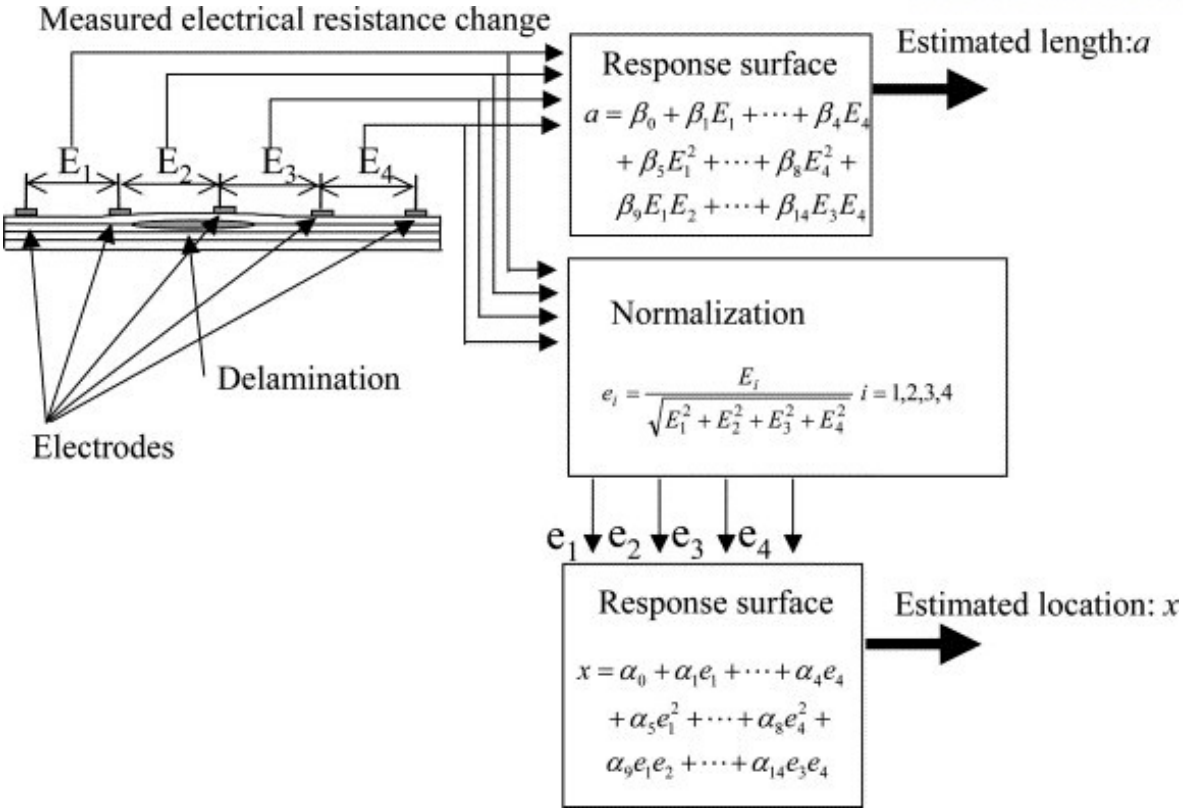

Fig. 2-4 Schematic diagram of electrical resistance change method for delamination detection[23]

J. Sebastian et al. suggested nanomaterial based sensor technique which makes it possible to detect the damages of wide area using fiber sensors covered by CNTs (fuzzy fiber). This fiber has good sensing performance exhibiting commensurate sensitivity with conventional metal strain gages (gage factor ~ 1.6-2.3) and advantages in that it can be easily integrated into composites as a sensor and composite in itself. The fuzzy fiber strain gages are able to respond to the various deformation modes such as the stimuli of longitudinal, transverse and off-axis orientation. The SEM image of fuzzy fiber sensor and its sensitivities are described in Fig. 2-5. [25]

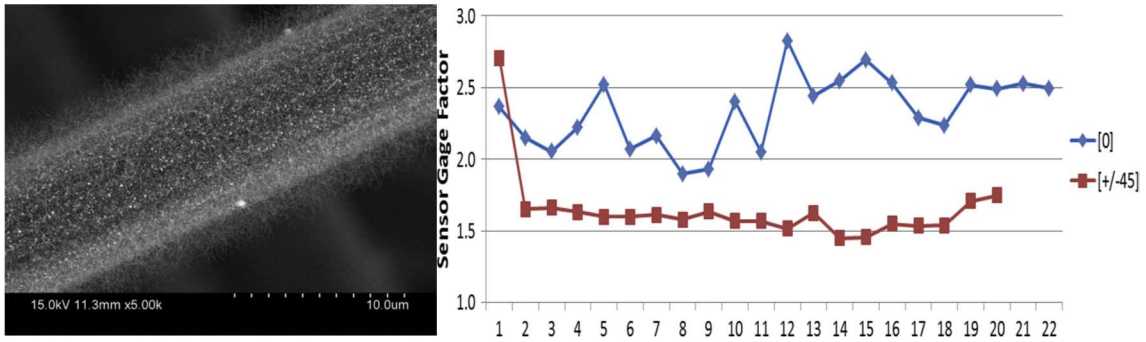

Fig. 2-5 SEM image of fuzzy fiber sensor and the sensor gage factor[25]

Self-healing polymers and fiber-reinforced polymer composites have the ability to heal for themselves when they undergo degradation, damage and failure. There are mainly three approaches classified in accordance with the mechanisms in which the healing agents are captured within the composites until triggered by stimuli: capsule based, vascular and intrinsic self-healing materials.[26] The work of J.F. Patrick et al. showed that repeated, in situ self-healing can be obtained in structural fiber-reinforced composites via microvascular delivery of sequestered, reactive healing agents. (Fig. 2-6) Sacrificial fiber technique formed vascular architectures in the composites and enabled those healing agents to be delivered. They tested healing performance with double cantilever beam fraction mode in order to embody the internal delamination. The group demonstrated the successful recovery of the fiber composite via three consecutive healing cycle. The larger loads were required to reinitiate the crack recovered.[27]

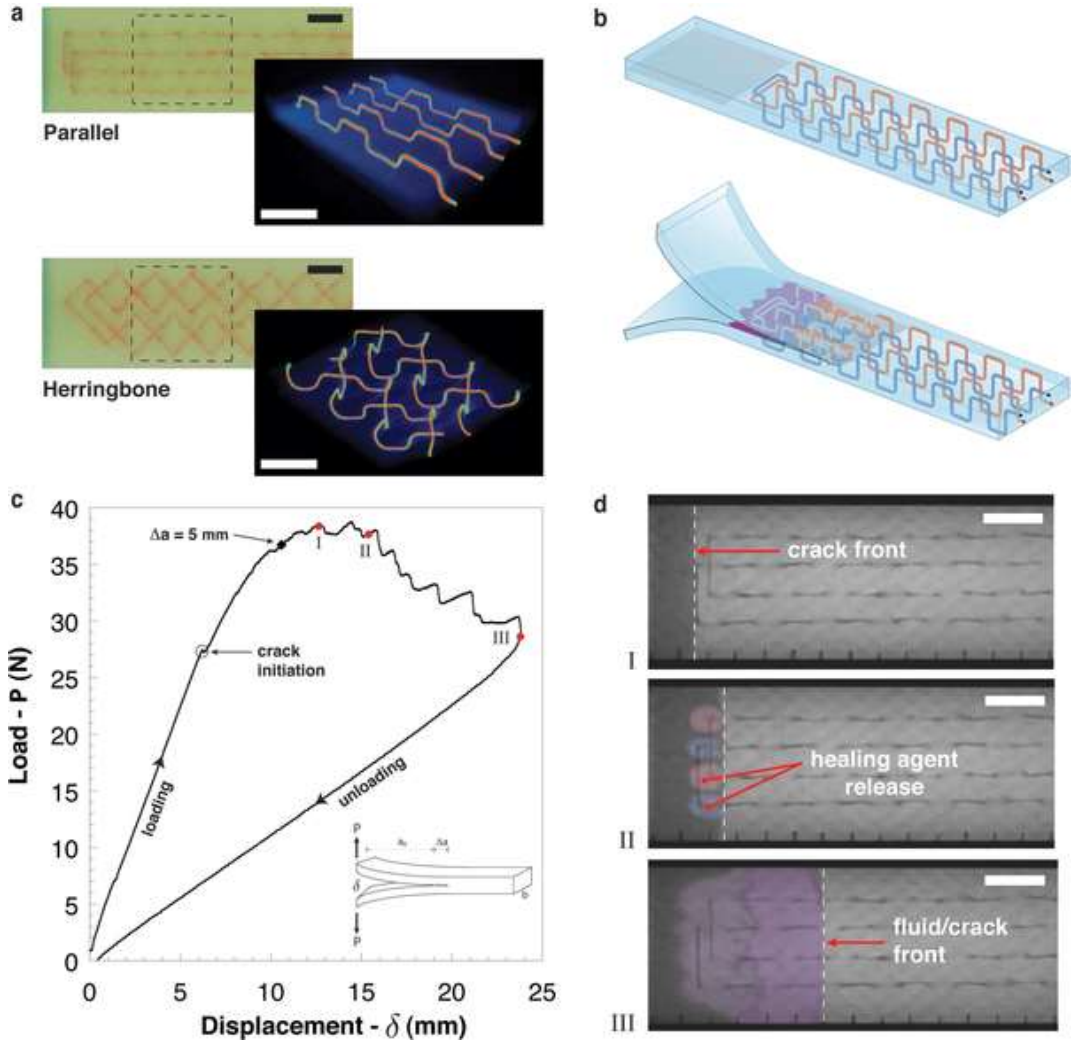

Fig. 2-6 In-situ healing agent delivery (a) Sacrificial fiber stitching patterns, (b) Schematic of microvascular double cantilever beam fracture specimen, (c) Representative load-displacement plot, (d) Optical transmission images of healing agent delivery[27]

2.3. Thermal and Electrical Conductivity Modeling of CNT-nanocomposites

Prediction and optimization of basic properties of composites have been required as above mentioned multi-functions have become of great importance. The modeling of the electrical conductivity and piezo sensing efficiency of nanocomposites for structural health monitoring is a representative example. If we know how the geometry, conductivity, etc. of CNT have an impact on the final electrical properties of a composite, it will be possible to design the module of piezo sensor whose sensitivity is optimized by calculating gage factor (ratio of relative change in electrical resistance to mechanical strain) under appropriate assumptions.

A great number of investigations on the thermal and electrical conductivities of CNT-nanocomposites have been developed using various modeling approaches, and introducing different conditions and assumptions. There are several general assumptions that many studies have imposed for the sake of simplicity of simulation: (1) perfect bonding between CNT fillers and polymer matrix, (2) fully dispersed fillers, (3) straightness of CNT and (4) random orientation. For the thermal conductivity of short fiber nanocomposites, micromechanics have been mainly used including Mori-Tanaka method, self-consistent method and interaction direct derivation method. In 1985, H. Hatta and M. Taya reported equivalent inclusion method which describes an ellipsoidal heterogeneity embedded into the matrix. The analysis takes account of the interaction among short fibers at different orientation via spherical coordinate transformation and distribution functions confining the angles of fibers.[28,29] C.-H. Chen. et al. also proposed the research on effective thermal conductivity of misoriented short-fiber composites. Mori-Tanaka's mean field theory was presented along with the Eshelby's equivalent inclusion method that takes the geometry of ellipsoidal inclusions into consideration. They demonstrated that thermal conductivity of composites relies on not only orientation distribution as H. Hatta did but also the length-diameter aspect ratio and the volume fraction of short fiber fillers.[30] Another research is the work of J. Yu that simulated effective thermal conductivity of CNT nanocomposites by means of micromechanics, Mori-Tanaka method and self-consistent method. Their modeling approaches accounted for the effect of orientation, agglomeration of CNTs and voids on resultant conductivity. They conducted the validation of their modeling results by comparing those with experimental results. Fig. 2-7 and 2-8 describe the comparison of the influences of CNT arrangement, voids included, and insulating agglomerates. The composites with aligned inclusions exhibited good thermal property since the carbon materials were dominant conducting filler despite their small amount. The voids and agglomerates of the fillers have diminishing effect on the movement of heat carriers.[31]

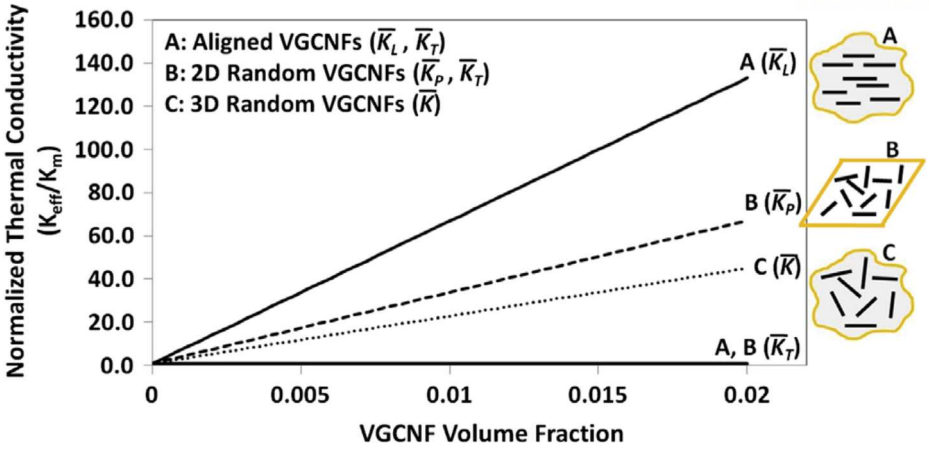

Fig. 2-7 Predicted thermal conductivities for vapor grown carbon nanofiber (VGCNF)/vinyl ester (VE) vs. filler volume fraction[31]

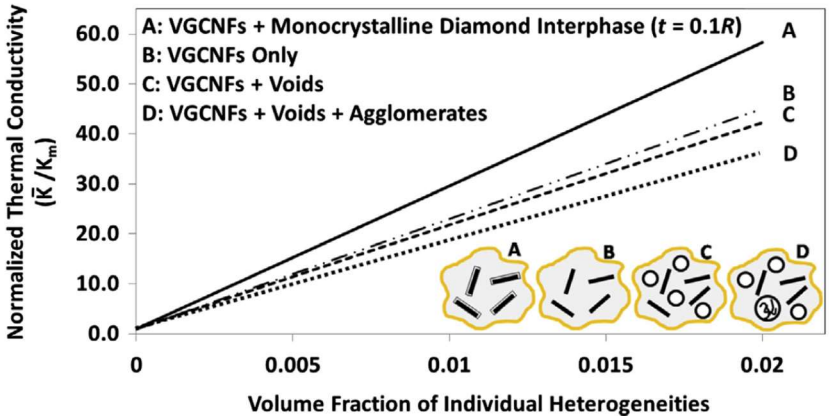

Fig. 2-8 Effect of various heterogeneities on effective thermal conductivities for VGCNF/VE[31]

In case of electrical conductivity modeling, there are more features we should consider, even though the governing equations for both thermal and electrical conductivity have the same form. The most notable aspect is percolation behavior which describes connected network of conducting fillers, in turn, electrical resistivity decreases drastically at the point called threshold. Indirect conducting mechanism is also seen in the CNT nanocomposites. It's called tunneling effect that an electron hops from one CNT to another one when the distance between the two CNTs is closer than the upper limit separation distance (~1.8nm) for CNTs but they don't come into direct contact with each other. Before dealing with the direct contact between two particles, interface effect is taken into account. K. Y. Yan et al. described the interface effect around the CNT with an average field theory to develop a model for effective electrical conductivity of CNT nanocomposites.[32] They reported that the increase of interface thickness made the percolation threshold become lower than that in the case of no interface effect. Another analytical model was proposed by F. Deng et al. The equation of percolation threshold called critical volume fraction in their work was developed regarding the aspect ratio, conductivity anisotropy and non-straightness of CNT.[33] There are several papers treating waviness or non-straightness of CNT. C. Li et al. focused on

the waviness of CNT which was approximated by elongated polygons. The fillers were selected by determining the positions of nodes whose consecutive gaps were fixed with constant segment length c. (Fig. 2-9) They applied direct electrifying algorithm and Monte Carlo simulation method to derived effective electrical conductivity. The results indicated that the composites with wavy CNTs had lower conductivity than that of straight CNT nanocomposites.[34]

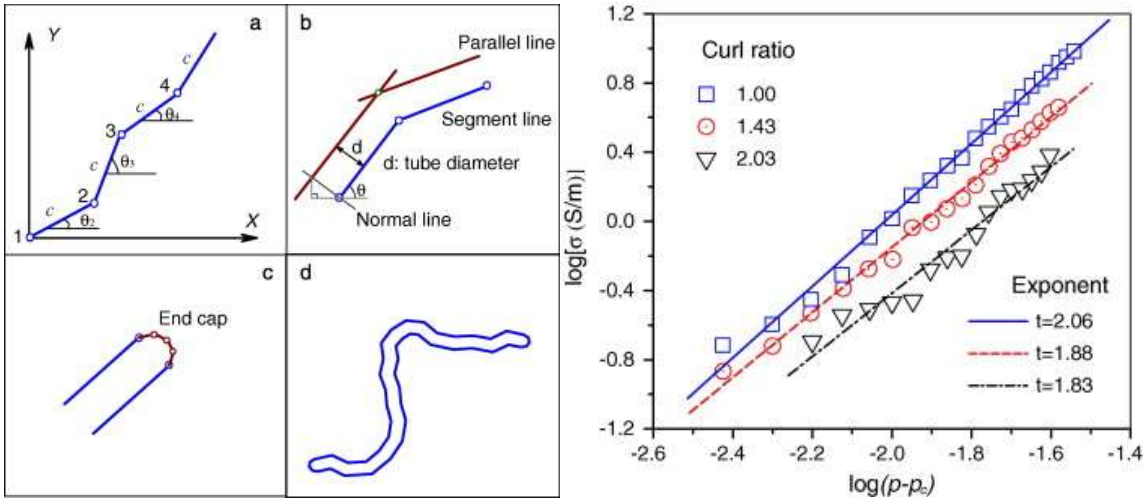

Fig. 2-9 Steps for wavy CNT and critical exponent of electrical conductivity[34]

The work of F. Dalmas et al. explained such decreasing tendency of conductivity. They investigated the influence of aspect ratio, tortuosity and fiber-fiber contact electrical properties on percolation threshold. They made similar tortuous CNT model in three dimensional space with the wavy CNT in C. Li et al.'s work. As the allowed tortuosity of fiber increased, the average fiber gyration radius decreased resulting in the increase of percolation threshold as described in Fig. 2-10. That is, it is unlikely to form conductive network between the dispersed CNTs when the CNTs are curved too much.[35]

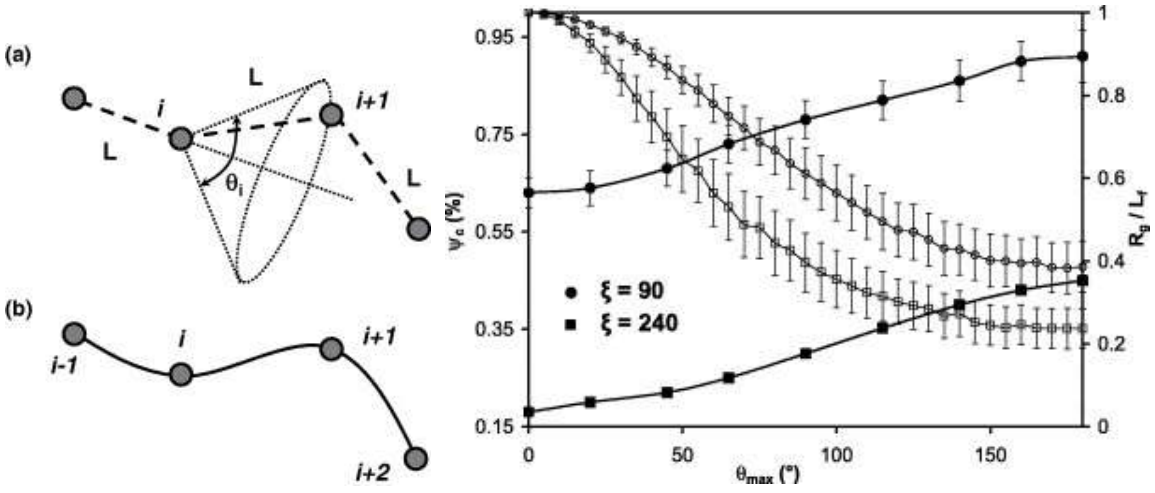

Fig. 2-10 Definition of wavy CNT and the simulated percolation threshold and the average fiber normalized gyration radius with the fiber tortuosity[35]

2.4. Thermal Conductivity Modeling of Woven Fabric Composites

Unlike the case of nanocomposites, electrical conductivity modeling methods of woven fabric composites have been seldom proposed whereas there are a considerable number of the prediction approaches of thermal conductivity. That is because the conducting mechanism of heat is comparatively less complicated than that of electricity and thermal-electrical analogy, a concept of heat transfer analysis, exists as a useful tool for investigating the relationship between woven fabric and polymer matrix.

Q.G. Ning et al. applied micromechanics models to simulate in-plane and through-thickness effective thermal conductivity of woven fabric composites.[36,37] A. Dasgupta et al.[38] and B. H. Seo et al.[39] also reported modeling approaches for the sake of the prediction of woven fiber composites' thermal conductivity. All of the papers dealing with thermal conductivity of woven fabric composites have something in common: (1) unit cell, (2) thermal-electrical analogy. One of the advantages of woven fabrics such as plain, satin and twill woven is repeatability of their geometry. The composites consisting of the woven fibers have a repeating element called unit cell which lets the researchers construct simple models to predict the effective conductivity of the composites, although the sizes of unit cells vary with the weaving method. Fig. 2-11 represents the way thermal-electrical analogy is applied to partitioned elements composing a unit cell in the work of B. H. Seo et al.

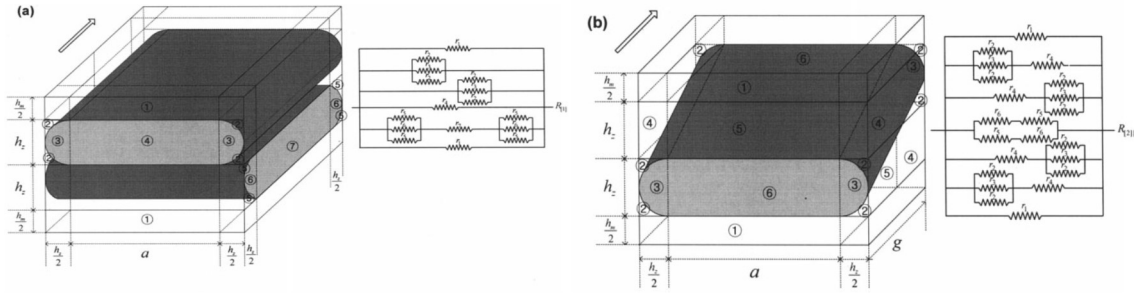

Fig. 2-11 Partitions and thermal resistance network of elements[39]

Each thermal resistance network has different form depending on the geometry of woven fibers or unit cells. This makes it cumbersome to set up the geometry of woven composites first and to divide the unit cell into elements with their own independent thermal resistance values.

2.5. Research Objectives

In an incremental step from scientific research to commercialization, poor thermal energy conversion performance is still an obstacle as figure of merit (ZT) of thermoelectric materials does not get over a certain value over the entire temperature range. Even if they are applied to practical life, additive devices on structures should make their geometry and combination design adjusted, which could be an extra burden. However, waste heat can be utilized without additional expense when thermoelectricity as a

multi-function is introduced to a structure that originally serves as only mechanical load-bearing part. Representative multi-functional composites are continuous fiber-reinforced composites and carbon nanocomposites. We will conduct studies on thermoelectric efficiency of multiscale and fiber reinforced composites whose constituents include CNT, CF, GF, and epoxy resin.

In this research, the proof-of-concept of using continuous woven fabric composites as thermoelectric materials has been demonstrated, which, to the best of our knowledge, has never been attemped. Two types of composites, namely, CNT/GF/epoxy composites and CF/epoxy composites are fabricated. Carbon substances develop conductive networks electrically within the composites whereas GF and epoxy polymer act as insulator in order to reduce thermal conductivity. Three intrinsic properties which figure of merit depends on, Seebeck coefficient, electrical conductivity and thermal conductivity, are empirically measured and the efficiency factors of each composite sample are obtained in terms of (1) the volume fraction of CNTs in multiscale composites, (2) the direction of exerted heat gradient, in-plane (IP) and through-thickness (TT) direction. In the process of Seebeck coefficient measurement, the coefficients of two types of composites will indicate which composite behaves like an n-type thermoelectric semiconductor or which one shows p-type thermoelectric behavior. After that, we will attempt to generate electric current when an electrical circuit is formed with two different composites.

In the latter half, we will investigate how the thermal and electrical conductivities of CNT/GF/epoxy and CF/epoxy composites vary with a range of variables that constituting substances have as a part of thermoelectricity optimization. Not only is it meaningful for the relevance to thermoelectricity, but also it will be an invaluable and challenging topic in that the prediction models are not enough which deal with the conductivity of multiscale composites and electrical conductivity of woven fabric composites as mentioned in Section 2.3 and 2.4. The core of multiscale composites' conductivity modeling is linkage between nanocomposite and woven fiber composite. That is the way in which effective conductivity value derived from nanocomposite's modeling is substituted for the conductivity of matrix in woven fabric composite modeling. It is quite powerful method in that it assures simplicity and makes the application scope of the model extended to a variety of other fields. Woven fabric composites' electrical conductivity model is embodied in the case of CF/epoxy composites. Mori-Tanaka model, a kind of the micromechanics, is taken, perceiving the prolate geometry of CF just like that of CNT. Finally, modeling approaches will be validated through comparison with empirical data.

Integrating the above approaches, it is anticipated that they open up the possibility of thermoelectricity as a multifunction of fiber composites and further researches on Seebeck coefficient of the composites make the calculation and optimization of thermoelectric efficiency possible. And proposing holistic approaches on the thermal and electrical conductivities of the polymer composites in which CNT or continuous fiber are impregnated will be expected beneficial to the composite manufacturing field.

3. Part 1: Evaluation of Thermoelectric Properties of Multifunctional Composites

3.1. Part Introduction

Characterization of thermoelectric properties of fiber filled composites has been reported by the author's research group.[40] Fig. 3-1 shows a schematic of a typical structure for a thermal energy harvesting system that has heat source and heat sink for heat absorption and release, respectively.[41] N-type and p-type thermoelectric materials transfer heat from the heat source to the heat sink while generating electric currents.[42] The objective of this research is to develop n-type and p-type thermoelectric materials using carbon nanomaterials, a polymer matrix, and commercial fibers, such as GF and CF. A three-roll mill and hand-layup process were employed to fabricate composite samples. A special test setup was designed to evaluate the thermoelectric performance of the samples. The electrical conductivity, thermal conductivity, Seebeck coefficient, and figure-of-merit (ZT) of the composite samples were evaluated. The developed composite structures could have multiple applications, including thermal energy harvesting devices as well as load carrying structures.

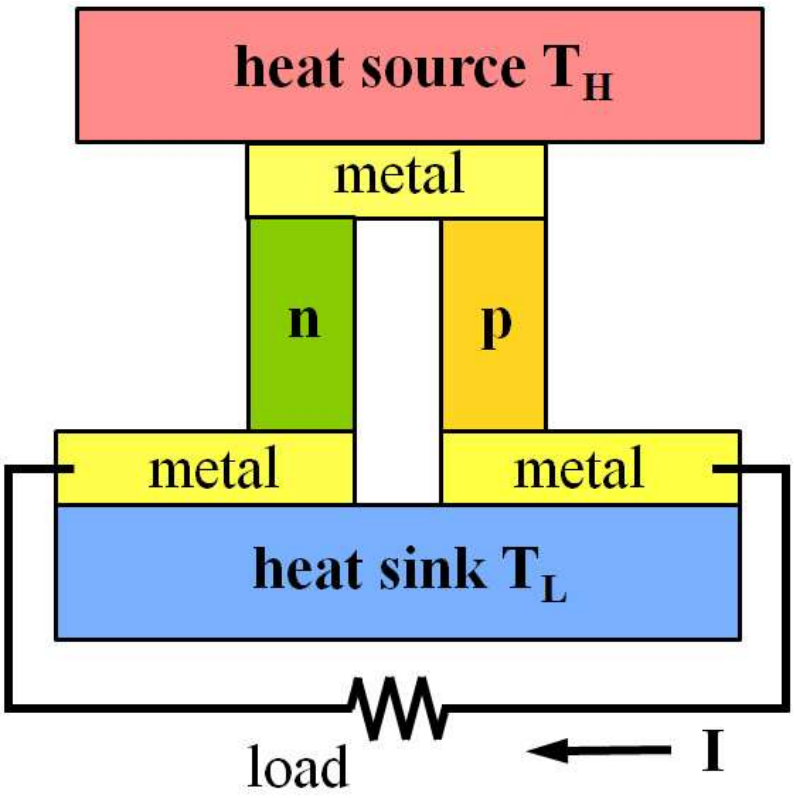

Fig. 3-1 The structure of a thermoelectric system for thermal energy harvesting

3.2. Experimental

3.2.1. Sample Preparation

CNTs used in this research were multiwall CNTs (MWCNTs, CM-100) provided by Hanwha Chemical, Korea. Plain-woven GF and CF (T300-grade) were employed for fiber reinforcement, and both were provided by JMC Co., Korea. The polymer matrix consisted of bisphenol-F type epoxy (YDF-170 from Kukdo Chemical Co., Korea) and a curing agent (SH- 101A from Sejin E&C, Korea).

Two types of samples were fabricated and tested: CNT/GF/epoxy multiscale composites and CF/epoxy composites. For the multiscale composite samples, the three constituent materials, pre-determined amounts of CNTs (0.5, 1, 3, 5 wt.%), epoxy resin, and curing agent were mixed in a container by manual stirring for 5 min followed by another mixing process using a paste mixer (PDM-300, Dahwa Tech Co., Yongin-si in Korea) (refer to Fig. 3-2). The revolution and rotation speeds of the paste mixer were 800 rpm and 640 rpm, respectively. The mixture ratio of the epoxy and curing agent was 100:25 by weight, which was the manufacturer-recommended composition. CNTs were dispersed in epoxy resin by a three-roll mill in the following step. The speed ratio of the three rollers was 1:3:9, and the third roller, the fastest roller, rotated at 270 rpm. CNT-epoxy mixtures were passed through the three-roll mill 10 times. After the dispersion process, CNT/GF/epoxy prepregs were prepared. As the first step in prepreg preparation, the CNT-epoxy mixture was poured on a plain-woven GF and then covered with a vacuum bag. The CNT-epoxy mixture was spread on the fabrics by manual pressing. The manufactured prepregs were placed on a hot plate for the hand-layup process and cured with curing and post-curing conditions of 120 °C for 2 h and 150 °C for 2 h, respectively. CF/epoxy composites were also fabricated using prepreg preparation and the hand-layup process. CF/epoxy prepregs were fabricated and cured on a hot plate using the same aforementioned curing and post-curing conditions. A copper plate was attached to each side of the composite sample. Copper plates were placed on top and bottom of impregnated fibers without any adhesives, such as glue, during the hand lay-up process. While being compressed by a vacuum bag, copper plates were fixed through epoxy curing. Since the contact area between copper plate and impregnated woven fibers was large enough and the manufacturing process involved vacuum-induced through-thickness compression, contact resistance was not taken into consideration.

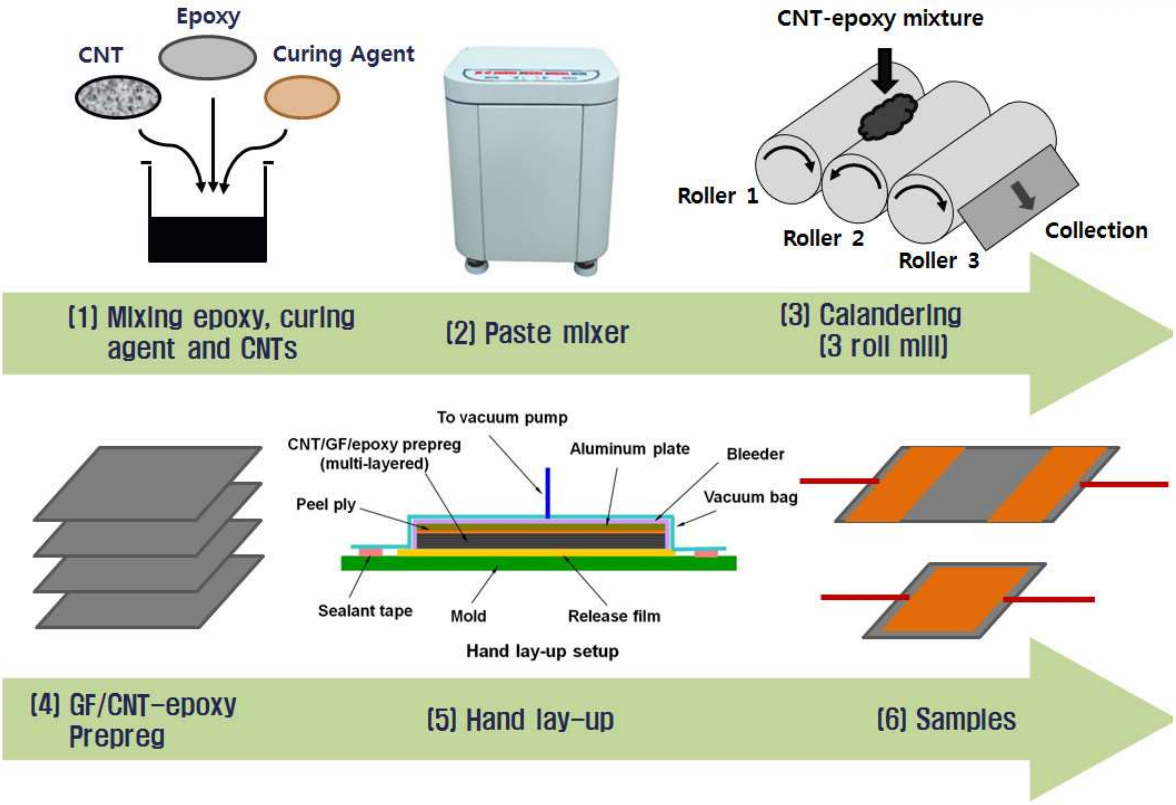

Fig. 3-2 Manufacturing process of multiscale composites

Fig. 3-3 shows a schematic for measuring voltage difference caused by temperature difference. As shown in Fig. 3-3(a), two different temperatures are applied to copper sheets on the left and right edges, and in-plane voltage differences were measured. For through-thickness voltage differences (Fig. 3-3(b)), temperature gradients were obtained by applying different temperatures at the top and bottom of the samples.

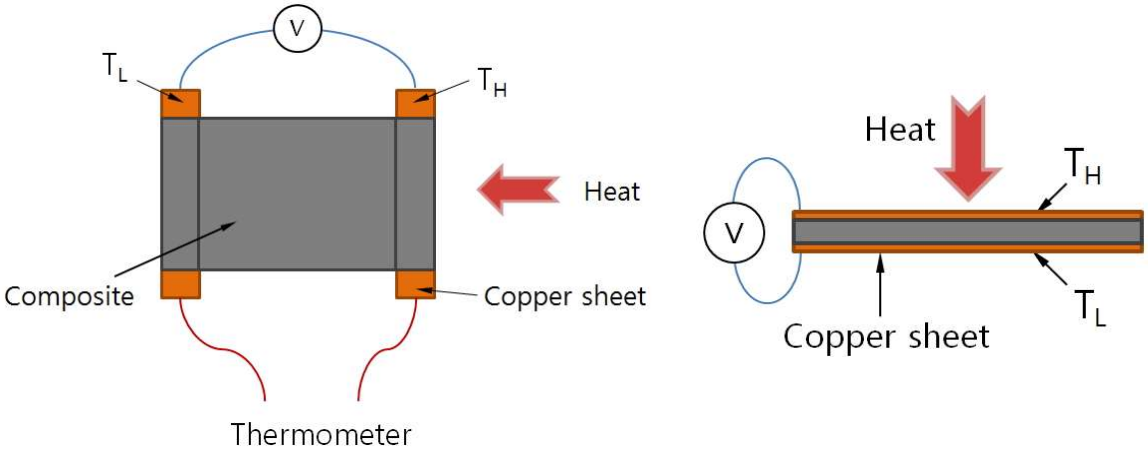

Fig. 3-3 Schematic of voltage measurement caused by temperature gradient: (a) in-plane voltage measurement, (b) through-thickness voltage measurement

Fig. 3-4 shows sample geometries for the in-plane measurement (Fig. 3-4(a)) and the through-thickness measurement (Fig. 3-4(b)). Low and high temperatures were applied to the left and right copper plates on in-plane samples, respectively, and the electronic voltages were measured by a multimeter connected to electric wires of the samples. For through-thickness samples, the temperature gradient was produced by low and high temperatures applied to the upper and lower copper plates of the samples, respectively. Eight layers and sixteen layers of woven fabric prepregs were used to make the in-plane and through-thickness samples, respectively.

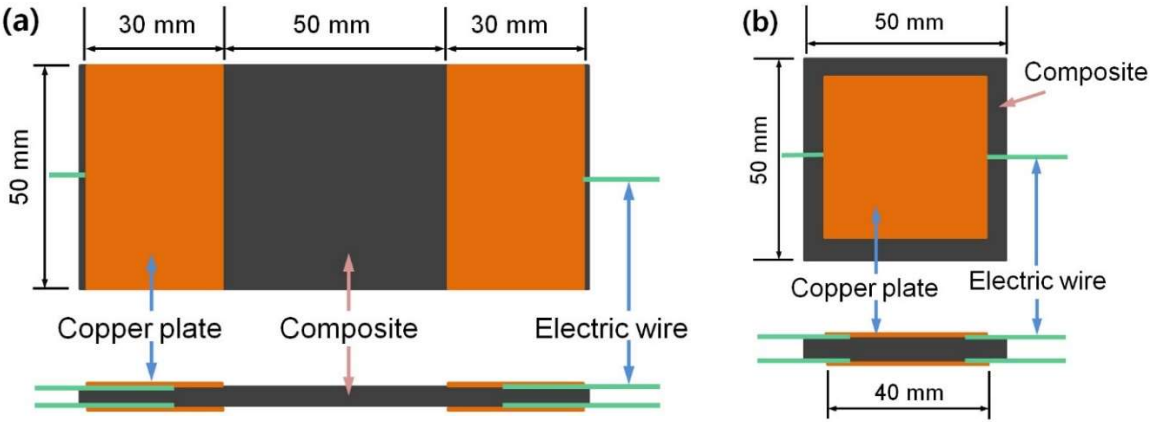

Fig. 3-4 Sample geometries for measuring thermoelectric properties: (a) in-plane voltage measurement, (b) through-thickness voltage measurement

3.2.2. Characterization

A special test setup with heating bars was developed in order to set the required temperatures of the composite samples for the characterization of the thermoelectric behavior. A multimeter (Model 2002, Keithley, U.S.A.) was used to measure the voltages created by temperature differences. Fig. 3-5(a) shows the test setup to measure the thermoelectric properties of the test samples. In-plane test samples were placed between heating bars controlled by the temperature control unit. The electric wires on a sample were connected to the multimeter to measure the voltage. The obtained voltage data were stored on a data collection computer in real time. Temperature control is the main issue in instrument calibration. A thermocouple was inserted into a heating bar and located behind the contacting surface between heating bar and sample so that sample temperature was accurately controlled.

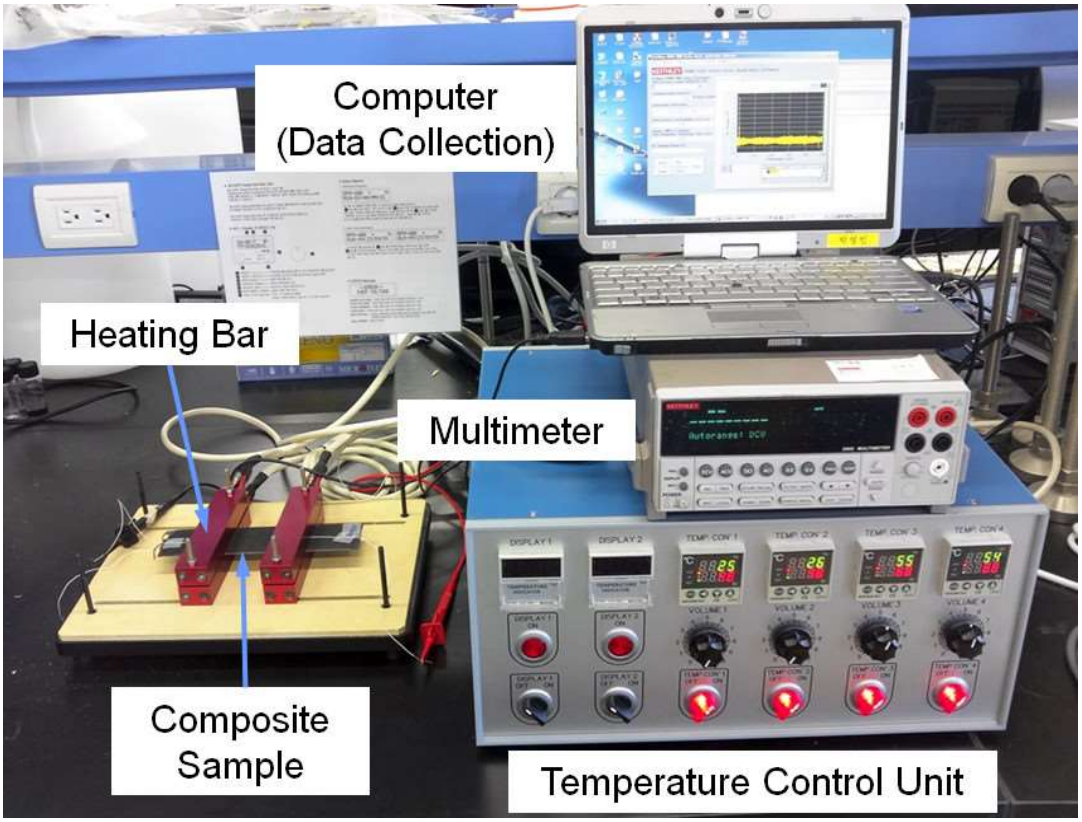

Fig. 3-5 Measurement setup for thermoelectric properties

The electrical conductivity of the samples were obtained indirectly using the electrical resistivity. The electrical resistivity of the samples were obtained at room temperature using the multimeter. A four-probe test was performed for in-plane samples, while a two probe test was performed for through-thickness samples because of the technical limitation created by the thin thickness. Contact resistance for the two-probe test may not be a significant issue in this case because the area of the copper plate probes was fairly large, 40 mm * 40 mm (refer to Fig. 3-4(b)).

Measurement of the thermal conductivity was performed using an LFA 447 manufactured by Netzsch, Germany. For the measurement of the in-plane thermal conductivity, test samples were cut to ~2.3 mm in width and ~13 mm in length and then placed vertically in a square holder, which was placed in the test machine. For the through-thickness thermal conductivity, the samples were cut in a circular shape with a diameter of ~12.7mm and then put in a holder placed in the test machine for the measurement.

3.3. Results and Discussion

3.3.1. Electrical Conductivity

An electrical conductivity of some material is a vital property for its thermoelectric application. As mentioned above, the electrical conductivity data were obtained from the electrical resistivity of the samples. Table 3-1 shows the conductivity and resistivity obtained by the four-probe method (for in-plane samples) and the two-probe method (for through-thickness samples). For the multiscale

composites consisting of CNTs, GF, and epoxy, the resistivity of the samples decreased as the content of CNT increased. The CF/ epoxy composite exhibited a relatively low resistivity due to high electrical conductivity of CFs, ~560 S/cm[43]. Another noticeable finding was that the resistivity of the in-plane samples showed lower resistivity than that of through-thickness samples. In the manufacturing process of prepregs, the CNT/epoxy mixture was poured on the woven GFs and then pressed manually and spread into the fibers. Therefore, most of the CNTs were in a two dimensional plane on the woven fabrics instead of aligned in the through-thickness direction, which is shown in Fig. 3-6. The white dots in the figure are CNTs cut during sample preparation by fracture. Many CNTs are shown to be partially aligned along the longitudinal fiber direction. The partially aligned CNTs on the woven fabrics are believed to have caused lower resistivity in the in-plane samples.

Table 3-1 Electrical resistivities and conductivities of the composite samples (IP: In-plane, TT: Through-thickness)

Sample	Electrical conductivity		Electrical resistivity	
	IP (S/m)	TT (S/m)	IP (Ω·cm)	TT (Ω·cm)
1 wt.% CNT/GF/epoxy	2.3669	0.1498	42.25 ± 0.010	667.4 ± 0.009
3 wt.% CNT/GF/epoxy	69.4444	0.9346	1.44 ± 0.002	107.0 ± 0.006
5 wt.% CNT/GF/epoxy	80.6452	1.4164	1.24 ± 0.002	70.6 ± 0.137
CF/epoxy	14705.8824	0.5675	0.00668 ± 1.04e-6	176.2 ± 0.895

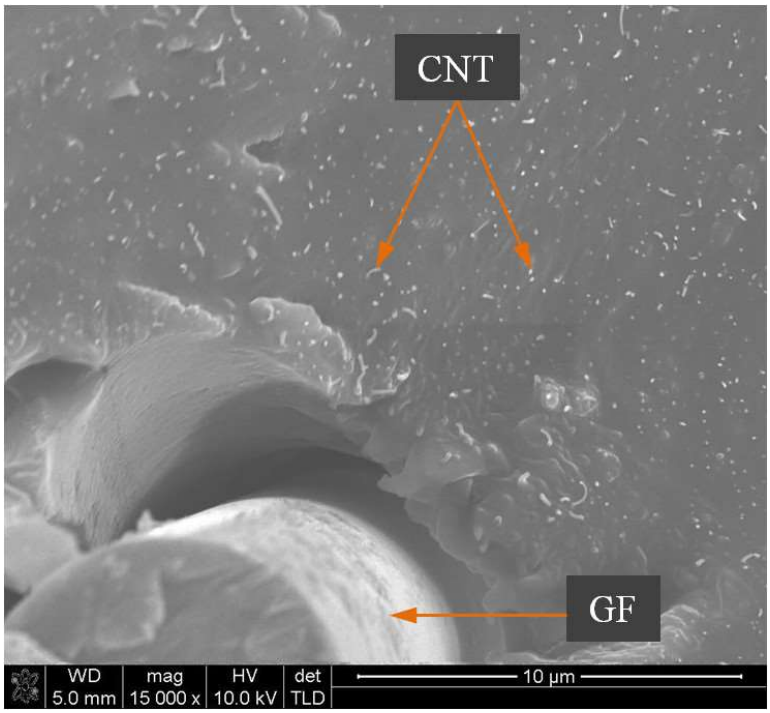

Fig. 3-6 SEM image of a 3 wt.% CNT/GF/Epoxy multiscale composite

3.3.2. Thermal Conductivity

Fig. 3-7 shows the in-plane and through-thickness thermal conductivities of the composite samples. Since CNTs have high thermal conductivity, the thermal conductivity of the multiscale composites increased as the CNT concentration increased. Similar to the electrical conductivity in Table 3-1, the in-plane thermal conductivity values of multiscale composites were higher than through-thickness thermal conductivity. The explanation for Fig. 3-6 in Section 3.3.1 can also be applied here. Partially aligned CNTs on the woven fabrics are believed to make the in-plane thermal conductivity higher than the through-thickness thermal conductivity.

In Fig. 3-7(a), the in-plane thermal conductivity of 0 wt.% CNT/GF/Epoxy is higher than that of 1 wt.%. The 0 wt.% sample has the advantage of better impregnation and compression due to the low viscosity of resin without CNT, and thus its fiber volume fraction was measured to be 5% more than that of the 1 wt.% sample. The more fiber are impregnated, the higher the thermal conductivity of composite, as the conductivities of GF and epoxy are 1.2-1.35 W/m-K and 0.19-0.22 W/m-K, respectively. In the case of thermal conductivity, percolation behavior induced by CNT network does not occur unlike electrical conductivity.[44] A CNT content of 1 wt.% only hinders the resin from flowing through GF and does not have a significant impact on composites' thermal conductivity.

The CF/epoxy composites showed a higher thermal conductivity than the CNT/GF/epoxy composites, which may be because of the following two reasons. One is that CF has a high thermal conductivity, and the other is that the CFs were continuous along in-plane direction but CNTs were discontinuous in the multiscale samples. Similar explanation can be applied between in-plane and through-thickness CF/epoxy samples, including continuity and discontinuity of fibers, respectively. CFs are discontinuous in through-thickness direction, which is the transverse direction of the fibers.

Thermal conductivity is a temperature-dependent property. The thermal conductivities of composite constituents, including CNT, CF, GF and epoxy vary with temperature. Kanari et al.[45] and Zhong et al.[46] demonstrated that the thermal conductivity of an amorphous polymer, especially epoxy, increases up to glass transition temperature as material temperature goes up. We used YDF-170 epoxy whose glass transition temperature is 162 °C which is higher than the temperature range of conductivity measurement in this paper. CNT, GF and CF also show increasing tendencies in thermal conductivity with increasing temperature due to activation of electrons.[47-49] The thermal conductivity of a composite derived from homogenization of constituents' properties must be increased in accordance with increasing conductivities of the components. Experimental data of Lin et al.[50], Park et al.[51] and Wan et al.[52] showed increases in thermal conductivities of composites with increasing temperature.

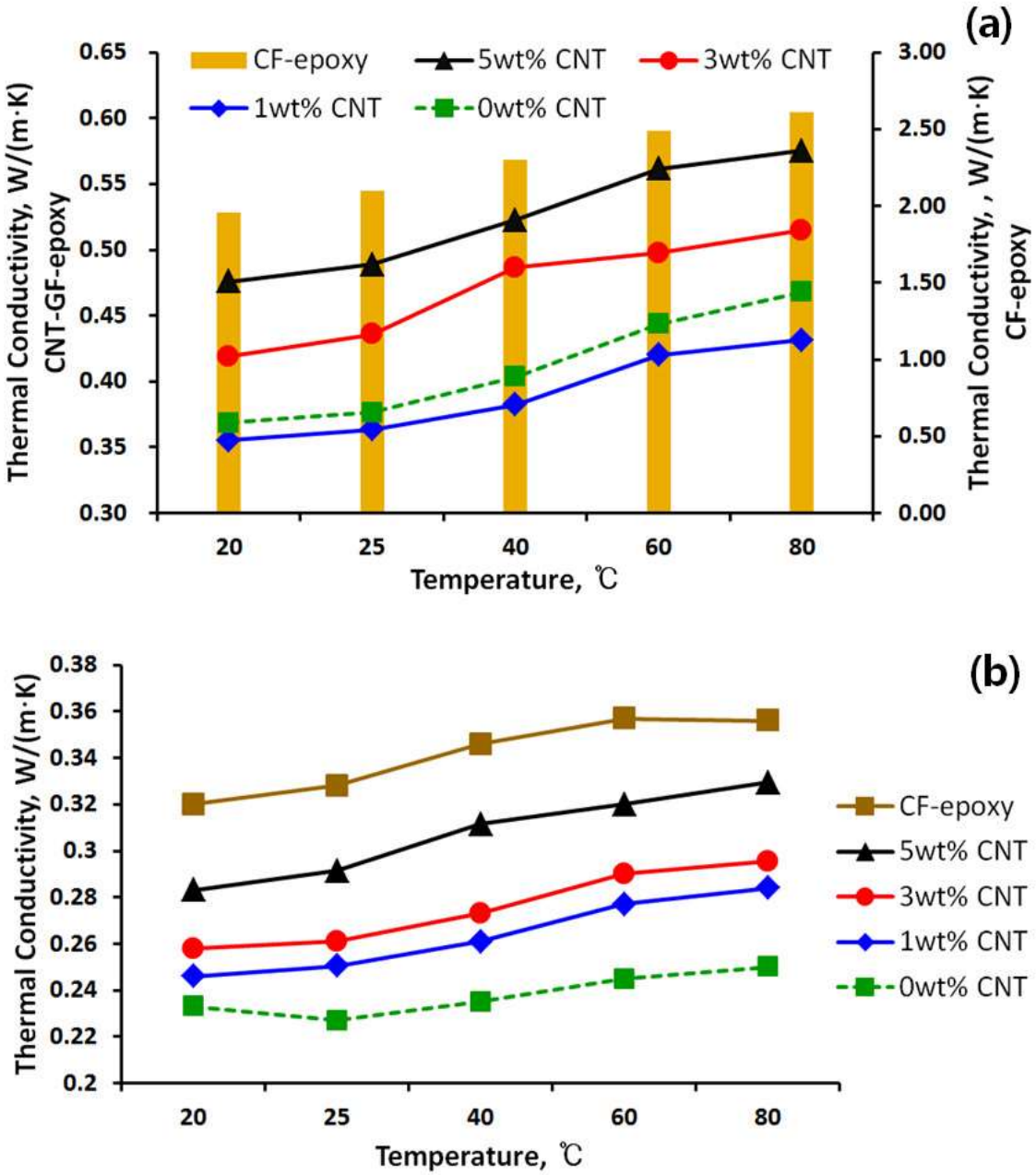

Fig. 18 Thermal conductivities of composite samples: (a) in-plane thermal conductivities, (b) through-thickness thermal conductivities of composite samples

3.3.3. Seebeck Coefficient

Seebeck coefficients were obtained by the voltage difference divided by the temperature difference ($\Delta V/\Delta T$).[53] Tables 3-2 and 3-3 present the Seebeck coefficients of the multiscale composites and CF/epoxy composite. As seen in the tables, the multiscale composites and CF/epoxy composite have negative and positive values, respectively. A negative Seebeck coefficient indicates a voltage drop in the direction from low temperature to high temperature, which is n-type thermoelectric behavior, whereas a positive Seebeck coefficient indicates a voltage drop in the opposite direction, which is p-

type thermoelectric behavior. Thus, with reference to Fig. 3-1, multiscale composites showed n-type thermoelectric behavior, while the CF/epoxy composite showed p-type thermoelectric behavior.

Table 3-2 Seebeck coefficients of the in-plane samples based on temperature differences

Left (°C)	Right (°C)	ΔT (°C)	1 wt.% CNT GF-EP(μV/°C)	3 wt.% CNT GF-EP(μV/°C)	5 wt.% CNT GF-EP(μV/°C)	CF-EP (μV/°C)
20	40	20	-5.731 ± 0.040	-4.940 ± 0.011	-6.163 ± 0.011	3.454 ± 0.026
20	60	40	-5.166 ± 0.021	-4.567 ± 0.014	-5.554 ± 0.007	4.033 ± 0.012
20	80	60	-5.056 ± 0.020	-4.532 ± 0.005	-5.708 ± 0.003	4.219 ± 0.009
40	60	20	-4.436 ± 0.156	-3.763 ± 0.011	-4.648 ± 0.011	3.945 ± 0.025
40	80	40	-4.749 ± 0.061	-4.173 ± 0.008	-5.456 ± 0.007	4.168 ± 0.011
60	80	20	-4.458 ± 0.039	-4.296 ± 0.016	-5.321 ± 0.013	4.175 ± 0.025
Average			-4.933	-4.378	-5.475	3.999

Table 3-3 Seebeck coefficients of the through-thickness samples based on temperature differences

Top (°C)	Bottom (°C)	ΔT (°C)	1 wt.% CNT GF-EP(μV/°C)	3 wt.% CNT GF-EP(μV/°C)	5 wt.% CNT GF-EP(μV/°C)	CF-EP (μV/°C)
20	40	20	-2.966 ± 0.014	-1.988 ± 0.058	-2.136 ± 0.015	1.953 ± 0.013
20	60	40	-2.939 ± 0.009	-2.026 ± 0.034	-2.228 ± 0.006	2.033 ± 0.013
20	80	60	-2.864 ± 0.018	-1.969 ± 0.018	-2.226 ± 0.019	1.983 ± 0.008
40	60	20	-2.935 ± 0.051	-1.860 ± 0.011	-2.060 ± 0.012	1.570 ± 0.023
40	80	40	-2.621 ± 0.010	-1.794 ±0.024	-1.981 ± 0.003	1.648 ± 0.018
60	80	20	-2.959 ± 0.028	-2.022 ± 0.036	-2.130 ± 0.049	1.605 ± 0.031
Average			-2.881	-1.943	-2.127	1.799

3.3.4. Figure-of-merit

The performance measurement of thermoelectric material is a figure-of-merit (ZT), which is the general expression of the efficiency of a thermoelectric material. The dimensionless figure-of merit is expressed as.[54]

$$ZT = \frac{\alpha^2 \sigma}{\kappa} T \quad (1)$$

where α, σ, and κ denote the Seebeck coefficient, electrical conductivity, and thermal conductivity, respectively. Fig. 3-8 shows the in-plane and through-thickness ZT values of the samples. Since in-plane samples had higher electrical conductivity than through-thickness samples (Section 3.3.1.), in-plane samples showed higher ZT values than those of through-thickness samples. The other two parameters, the Seebeck coefficient and thermal conductivity, did not show significant differences between in-plane and through-thickness samples. In the in-plane ZT in Fig. 3-8(a), the CF/epoxy composite showed a higher ZT than the multiscale composites because of the high electrical conductivity and continuity of CFs. However, the through-thickness ZT of the CF/epoxy showed a

lower ZT than that of the 3 or 5 wt.% CNT composite samples. Some of the CNTs in the multiscale composites were aligned in through-thickness direction, leading to higher Seebeck coefficients and electrical conductivity in 3 and 5 wt.% CNT samples (Table 3-1).

Even though the ZT values in Fig. 3-8 are low for commercial applications, we believe that the values can be improved by forming segregated-network CNTs in the composites and increasing the CNT weight fraction.[16]

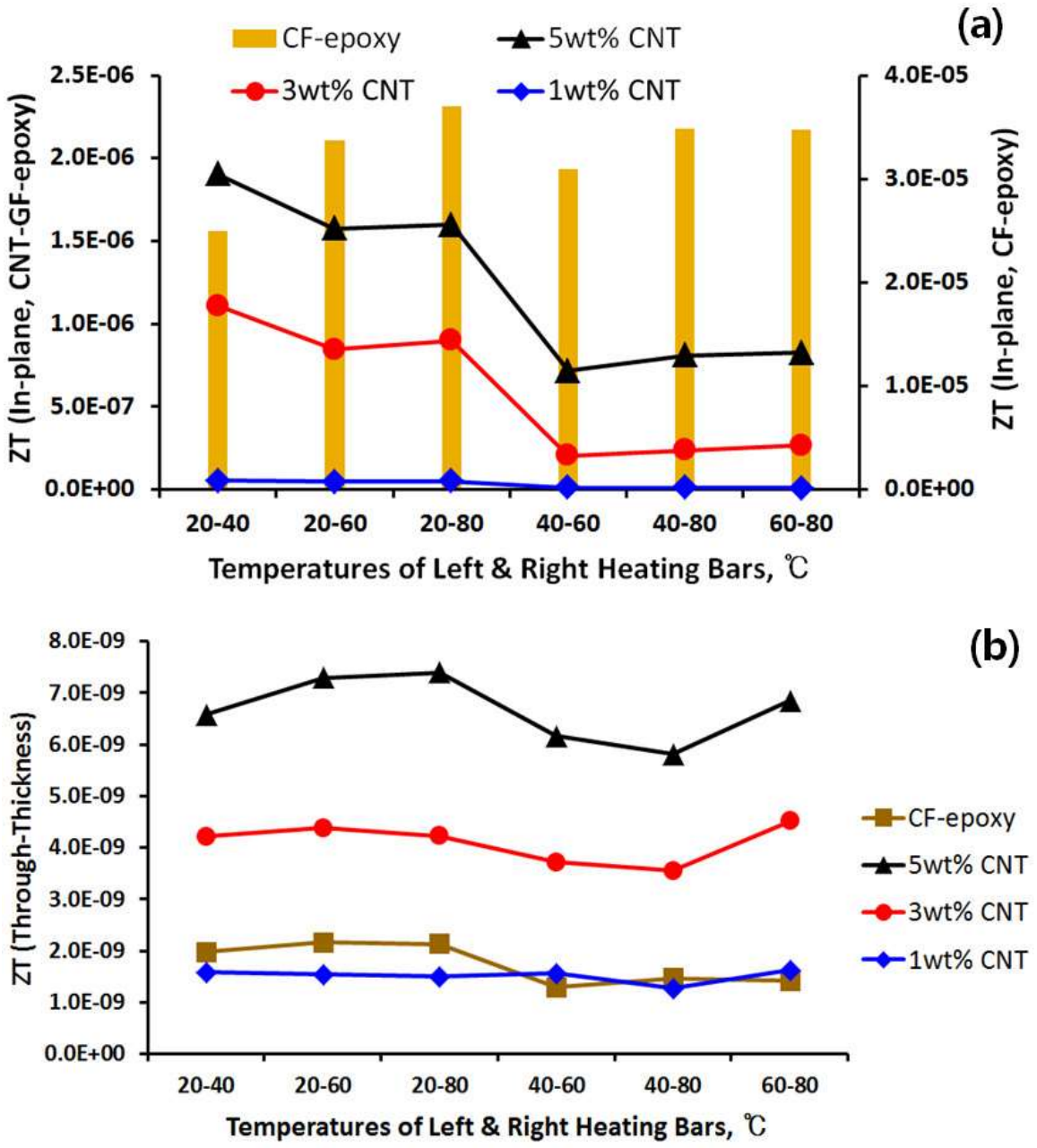

Fig. 3-8 Figure of merits (ZTs) of the composite samples: (a) in-plane, (b) through-thickness

3.3.5. Thermal Energy Harvesting

Thermal energy harvesting is a technology for generating electricity by transferring waste heat from a heat source to a heat sink through n/p thermoelectric materials, as shown in Fig. 3-1. Fig. 3-9 shows an energy harvesting system comprised of multiscale and fiber-reinforced composites. Based on the results in Section 3.3.3, the CNT/GF/epoxy multiscale composites and CF/epoxy composite were used as n-and p-type thermoelectric materials, respectively. Probes 1 and 2 were connected to the multimeter in order to measure the electric current. Fig. 3-9(a) shows a schematic of in-plane energy harvesting with low temperature at the left heating bars (bar 1 and 2) and high temperature at the right heating bars (bar 3 and 4). Insulation material separated the multiscale composite from the lower heating bars for heat insulation and electric transfer between them. Compared with Fig. 3-1, electric current flows from left to right in the CNT/GF/epoxy composite, whereas the current flows from right to left in CF/epoxy composite. Thus, the electric current flows in the clockwise direction. When the connecting positions of probes 1 and 2 to the multimeter were exchanged, the multimeter indicated negative values. This proved that the electric current flows in the specified direction. Fig. 3-9(b) illustrates energy harvesting with through-thickness composite samples. Higher and lower temperatures were set at the heating bars above and below the composite samples, respectively. In case of in-plane energy harvesting, CF/epoxy sample acted as the p-type material, in which positive holes transferred heat from heating bar 4 to 2, while multiscale composite acted as the n-type material, in which electrons transferred heat from heating bar 3 to 1.

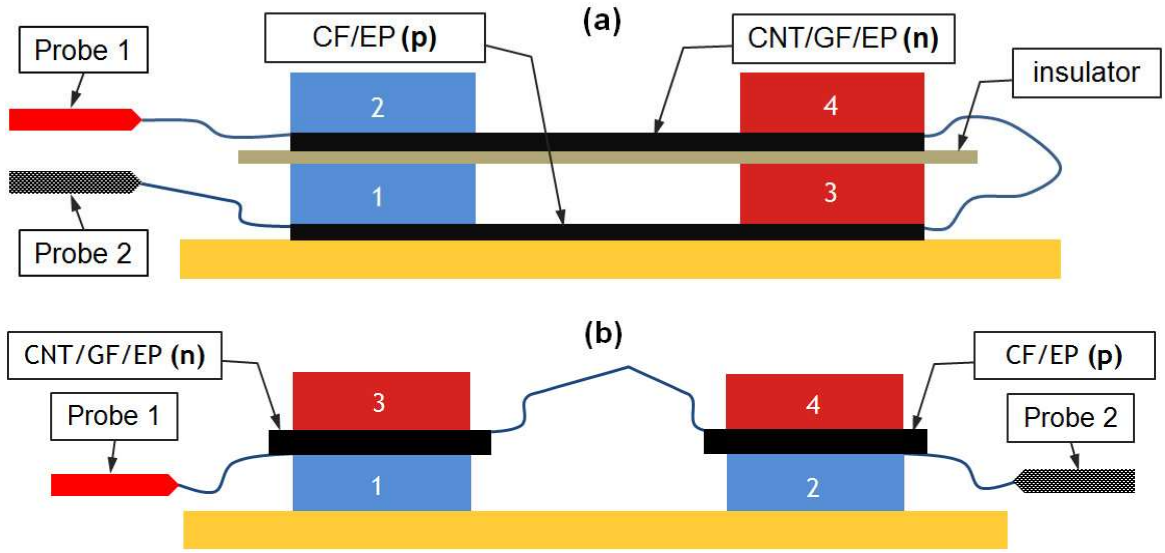

Fig. 3-9 Thermal energy harvesting: (a) in-plane direction (b) through-thickness direction

Tables 3-4 and 3-5 show the generated electric current based on the temperature differences. As the CNT concentration increased, the generated electric current increased. As shown in Fig. 3-8, the ZT of the multiscale composites, a measurement of thermoelectric performance, increased as the CNT

concentration increased. Similar to the results for ZT, the values of the electric current seem insufficient for industrial applications of thermal energy harvesting. Electric current generation, however, can be enhanced by structural optimization, such as maximizing the current generation using composites with a proper ZT and/or employing a multilayer arrangement of the composites. Nevertheless, this study demonstrated the possibility and provides the foundation for the further development of lightweight, low-cost, and nontoxic multifunctional composites for thermal energy harvesting in the future.

Table 3-4 Generated electric current with in-plane samples based on temperature differences

Temperature (℃)			Current (nA)		
Left (1,2)	Right (3,4)	ΔT	1.0 wt.%	3.0 wt.%	5.0 wt.%
20	40	20	128.2 ± 2.3	176.6 ± 3.8	202.4 ± 0.4
20	60	40	258.2 ± 2.9	316.8 ± 0.3	377.8 ± 0.3
20	80	60	418.3 ± 3.7	474.7 ± 0.3	566.9 ± 0.4
40	60	20	114.8 ± 2.7	124.4 ± 0.5	142.1 ± 0.4
40	80	40	244.1 ± 6.9	279.9 ± 0.5	341.3 ± 0.8
60	80	20	104.8 ± 2.4	135.8 ± 0.6	146.7 ± 0.6

Table 3-5 Generated electric current with through-thickness samples based on temperature differences

Temperature (℃)			Current (nA)		
Bottom (1,2)	Top (3,4)	ΔT	1.0 wt.%	3.0 wt.%	5.0 wt.%
20	40	20	132.2 ± 0.3	87.0 ± 0.7	107.0 ± 0.4
20	60	40	253.4 ± 0.5	163.0 ± 0.7	216.0 ± 0.5
20	80	60	389.6 ± 0.7	239.5 ± 0.9	334.9 ± 0.8
40	60	20	113.3 ± 0.5	88.5 ± 0.6	96.3 ± 0.7
40	80	40	242.7 ± 0.5	191.6 ± 0.5	209.0 ± 0.5
60	80	20	123.6 ± 0.6	110.8 ± 0.9	113.1 ± 0.9

3.4. Summary

CNT/GF/epoxy and CF/epoxy composites were fabricated and characterized to investigate their thermoelectric properties and potential for thermal energy harvesting and load carrying structural composites. A calendaring process was used to disperse CNTs in epoxy, and a hand-layup process was employed to manufacture fiber-reinforced composites. The electrical conductivity, thermal conductivity, and Seebeck coefficient were measured to obtain figure-of-merit (ZT) of composite samples, which is a measure of thermoelectric efficiency. A special test setup was developed to obtain the Seebeck coefficient. In-plane samples showed higher electrical and thermal conductivity because of the partial alignment of CNTs and continuity of CFs within the plane. In general, CF/epoxy composites had better electrical and thermal conductivities than those of the multiscale composites. In the Seebeck coefficient test, CNT/GF/epoxy composites showed n-type thermoelectric behavior, while CF/epoxy composites exhibited p-type thermoelectric behavior. The closed loop electrical circuit comprised of the developed composites generated electric current successfully in the presence of temperature gradient. However,

for the sake of commercial applications of the composites, the figure-of-merit (ZT) should be improved, and the module structure should be optimized by forming segregated-CNT networks in the composites and employing multilayer arrangements of the composites. This study is expected to be the basis for further development of lightweight, low-cost, and nontoxic multifunctional composites for thermal energy harvesting in the future.

4. Part 2: Conductivity Modeling for Optimizing Thermoelectric Efficiency

4.1. Part Introduction

The goal of this part is to propose analytical approaches to predict the thermal and electrical conductivities of CNT/GF/epoxy multiscale composites and CF/epoxy composites with respect to the variables of constituents. As the first step, electrical and thermal conductivities of nanocomposites were obtained using the Mori-Tanaka methods the works of C. Feng et al.[55] and J. Yu et al.[31] respectively, and then the obtained conductivities were employed as the matrix properties in the woven fabric composite model in order to make the composites multiscale. Thermal-electrical analogy was applied to thermal conductivity analysis of woven fabric composites, whose geometry was defined by sinusoidal function following the work of D. Scida et al.[56] For electrical conductivities of woven fabrics composites, Rule of mixture in which an effective cross-sectional area was introduced and modified Mori-Tanaka method that nanocomposite conductivity model follows were employed and the results of both methods were compared with each other. Finally, analytical modeling results were validated by drawing a comparison with empirical data.

4.2. Methods

4.2.1. Modeling Procedure

In this numerical modeling and experiment, multiscale composites were composed of plain-woven GF, CNTs and epoxy resin. Fiber reinforced composites consist of plain-woven CF and epoxy. Fig. 4-1 shows overall conductivity modeling procedure of the composite materials. Multiscale composites were subjected to both nanocomposite and woven fabric composite modeling whereas the modeling of fiber-reinforced composites didn't need the nanocomposite modeling procedure. Effective properties of CNTs and epoxy matrix were obtained by nanocomposite modeling that used Mori-Tanaka method (MTM), one of micromechanics. The obtained nanocomposites properties were used as matrix conductivities in woven fabric composite modeling, which calculated effective conductivity of composite containing two constituents, woven fiber and matrix.

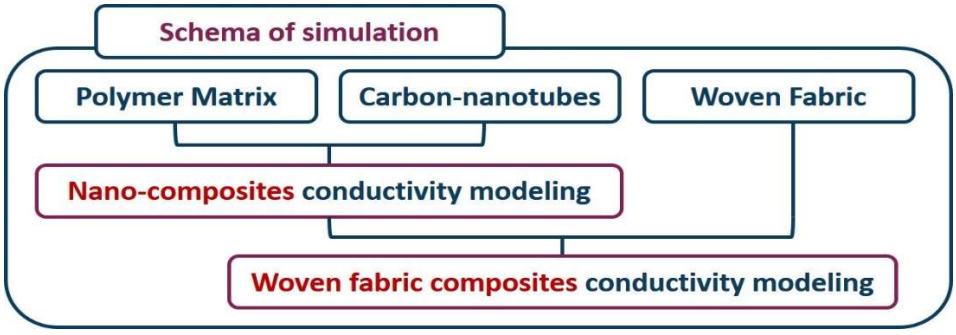

Fig. 4-1 Schema of overall modeling procedure

4.2.1.1. Nanocomposite Modeling

Prediction of nanocomposite conductivity refers to that of mixture between CNTs and epoxy polymer matrix using MTM equations, which are from the papers of Yu et al. [31] and Feng et al. [55] in thermal and electrical conductivity, respectively. For both thermal and electrical conductivity modeling, MTM considered an ellipsoidal heterogeneity inserted into the matrix which was subjected to the infinite flux and included Eshelby tensor that explained an influence of the filler's aspect ratio (A_r). For the sake of simplicity, it was assumed that CNTs are straight and perfectly dispersed within the matrix. Eshelby tensor was defined as equation (2) since a CNT has prolate geometry in z-direction. [57]

$$S = \begin{bmatrix} S_{11} & 0 & 0 \\ 0 & S_{22} & 0 \\ 0 & 0 & S_{33} \end{bmatrix}$$
$$S_{11} = S_{22} = \frac{A_r}{2(A_r^2 - 1)^{3/2}}\left[A_r (A_r^2 - 1)^{1/2} - \cosh^{-1} A_r\right] \tag{2}$$
$$S_{33} = 1 - S_{11}$$

Using coordinate transformation matrix (3), it was possible to consider the effect of CNTs' orientation either random or aligned arrangement. Volume average was introduced to derive mean value of a matrix transformed from local to global coordinate as shown in (4) and (5).

$$Q = \begin{bmatrix} \cos(\psi)\cos(\varphi) & \sin(\psi)\cos(\varphi) & -\sin(\varphi) \\ -\sin(\psi) & \cos(\psi) & 0 \\ \cos(\psi)\sin(\varphi) & \sin(\psi)\sin(\varphi) & \cos(\varphi) \end{bmatrix} \tag{3}$$

$$A = Q^T \tilde{A} Q \tag{4}$$

$$\overline{A} = \frac{1}{V}\int_0^{2\pi}\int_0^{\pi} A \sin(\varphi) d\varphi d\psi \tag{5}$$

Even though the same method (MTM) is applied to both thermal and electrical conductivities, their conducting mechanisms are so different from each other that the conductivity variations showed quite different tendencies between them in terms of volume fraction of filler. Electrical conductivity is affected by direct ohmic contact and indirect tunneling effect and therefore it has percolation behavior. However, such a drastic change doesn't occur in case of thermal conductivity with respect to volume fraction but it shows almost linear change.

Equation (6) is a governing equation for thermal conductivity which is defined by far field heat flux and mean temperature gradient.[31]

$$q = \overline{K} \cdot (-\nabla T) \tag{6}$$

Effective thermal conductivity constituted with matrix phase and heterogeneity is represented by equations (7) and (8).[31]

$$K_{eff} = K_m : \left\{ I + \sum_i^N f_i (S_i - I) : (A_i - S_i)^{-1} \right\} : \left\{ I + \sum_i^N f_i S_i : (A_i - S_i)^{-1} \right\} \tag{7}$$

$$A_i = (K_m - K_i)^{-1} : K_m \tag{8}$$

where A_i is the second-rank concentration tensor for CNT. K_m, K_i are the second-rank thermal conductivity of matrix and i-th CNT. f_i is volume fraction of the fillers and *S* is second-rank Eshelby tensor for CNT. *I* is second order identity tensor and a colon (:) represents double dot product of second order tensor, respectively.

Governing equation of electrical conductivity has similar form to that of thermal conductivity with current density and electrical field.[58]

$$J = \overline{\sigma} \cdot E \tag{9}$$

Effective electrical conductivity containing N of heterogeneities and matrix is determined by below equations (10) through (12).[58]

$$\sigma_{eff} = \sigma_m + \sum_i^N f_i (\sigma_i - \sigma_m) \cdot A_i \tag{10}$$

$$A_i = T_i \cdot \left[f_m I + \sum_j^N f_j T_j \right]^{-1} \tag{11}$$

$$T_i = \left[I + S \cdot \sigma_m^{-1} \cdot (\sigma_i - \sigma_m) \right]^{-1} \tag{12}$$

A_i is the second-rank electrical field concentration tensor for CNT. σ_m, σ_i are the second-rank electrical conductivity tensors of matrix and *i-th* CNT. f_i and S denote the volume fraction of fillers and the second-rank Eshelby tensor for CNT, respectively.

There were two different features from thermal conductivity. First, interface shell was introduced and defined, and second, conductive mechanism was divided into electron hopping and conductive network formation which in turn tunneling effect could be introduced. In case of conductive network formation, the network was regarded to be formed by infinitely long CNTs.[58]

4.2.1.2. Woven Fabric Composite Thermal Conductivity Modeling

Conductivity modeling of woven fabric composites covered CNT/GF/epoxy multiscale composites and CF/epoxy fiber-reinforced composites. It dealt with the relationship between woven fabric and matrix like CF and epoxy in fiber-reinforced composite. In case of multiscale composite with GF, CNTs, and epoxy, the matrix properties were replaced by the effective conductivities from nanocomposite modeling. Modeling methods of thermal and electrical conductivities also had difference due to similar reason with the difference between thermal and electrical conductivity modellings for nanocomposites. Effective thermal conductivity values were obtained by using thermal-electrical analogy, whereas effective electrical conductivities were calculated by rule-of-mixtures (ROM) and Mori-Tanaka method (MTM), which was utilized for nanocomposites.

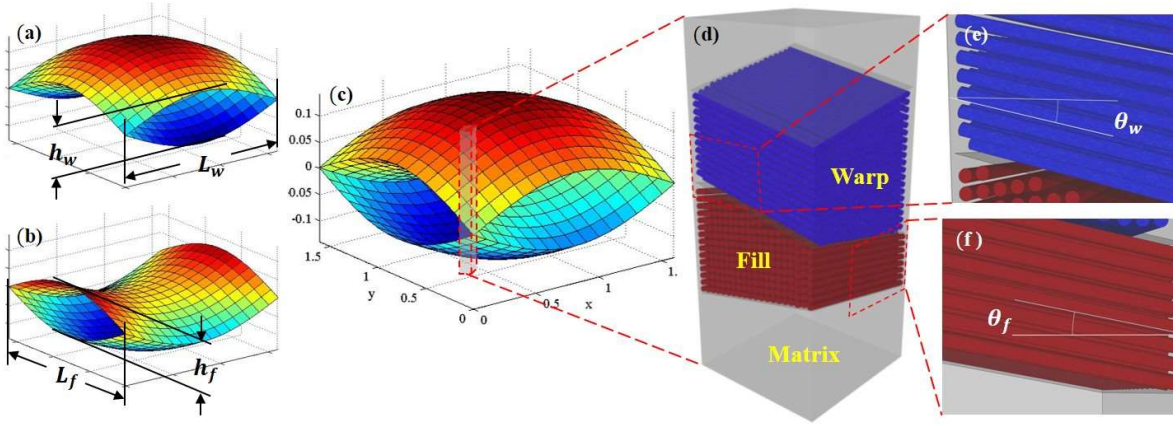

Fig. 4-2 Thermal conductivity modeling scheme of woven fabric composites

Plain woven fabric composite whose repeating unit cell is shown in Fig. 4-2(a-c) were selected to study fiber-reinforced composites. Thermal-electrical analogy was applied to this unit cell when the cell was divided into identical rectangular parallelepiped elements into which resistance values were allocated. Effective thermal conductivity was deduced by comparing resultant resistance calculated by forming circuit with every element resistance and total resistance. Equation (13) and (14) represent how the resistances were obtained.

$$R_i = \frac{L_i}{K_i S_i} (i = 1,2,...,N) \tag{13}$$

$$R = \frac{L}{K_{eff} S} = \left[\sum_{j=1}^{N_p} \left(\sum_{i=1}^{N_s} R_i \right)_j^{-1} \right]^{-1} \tag{14}$$

R_i denotes the thermal resistance of each element in certain direction and was calculated with its

conductivity, length and cross-sectional area. R, L, S, K_{eff} were, respectively, total resistance, length, cross-sectional area, and effective thermal conductivity of unit cell. (Fig. 4-3)

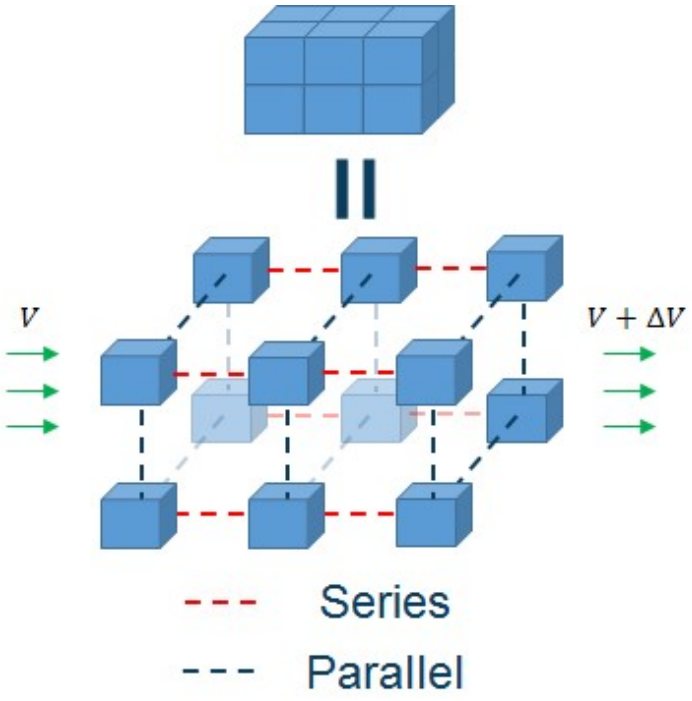

Fig. 4-3 Thermal-electrical analogy

Geometry of unit cell was defined by sinusoidal functions with undulation and fiber tow thickness in order for thermal resistance of each elements. [56]

$$H_f(x) = -\frac{h_w}{2}\sin\left(\frac{\pi x}{L_w}\right) \qquad 0 \le x \le L_w \tag{15}$$

$$e_f(y) = \frac{h_f}{2}\sin\left(\frac{\pi y}{L_f}\right) \qquad 0 \le y \le L_f \tag{16}$$

$$H_w(y) = \frac{h_f}{2}\sin\left(\frac{\pi y}{L_f}\right) \qquad 0 \le y \le L_f \tag{17}$$

$$e_w(x) = \frac{h_w}{2}\sin\left(\frac{\pi x}{L_w}\right) \qquad 0 \le x \le L_w \tag{18}$$

In above equations, *H, e, h, L* denote undulation, thickness variation, tow maximum thickness, and strand width, respectively. Subscripts f and w represent fill and warp strand, respectively. (Fig. 4-2 (a,b))

The unit cell with size of $L_f \times L_w \times (h_f + h_w)$ was divided into elements of $dx \times dy \times dz$ which have their own resistance values corresponding to their location. The resistance values vary with conducting direction, type and angle of fabric at each location.

As the first step for obtaining thermal conductivity, the concept of impregnated strand should be defined. As shown in Fig. 4-2(d), a unit cell consists of matrix, fill and warp strand regions. Fill and warp strand regions were not comprised of dry filaments but filled with the filaments impregnated by epoxy matrix. Therefore, fiber volume fraction of each region called impregnated fiber volume fraction was different from that of unit cell and needed to be recalculated. Equation (19) shows how impregnated volume fraction was derived. The axial and transverse conductivities of impregnated tow were obtained from Rule of mixture and Clayton's definition. (Equations (20), (21))[36,59,60]

$$f_{ip} = f\frac{V}{2V_{ip}} \tag{19}$$

where $V = L_w \times L_f \times \left(h_w + h_f\right),\ V_{ip} = L_w \times 2\int_0^{L_f} e_f(y)dy$

$$K_{a,ip} = f_{ip}K_a + (1 - f_{ip})K_m \tag{20}$$

$$K_{t,ip} = \frac{K_m}{4}\left[\sqrt{\left(1 - f_{ip}\right)^2\left(\frac{K_t}{K_m} - 1\right)^2 + \frac{4K_t}{K_m}} - \left(1 - f_{ip}\right)\left(\frac{K_t}{K_m} - 1\right)\right]^2 \tag{21}$$

K_a, K_t and K_m represent the thermal conductivities of axial and transverse direction of filament and matrix, respectively. $K_{a,ip}$ and $K_{t,ip}$ denote the thermal properties of impregnated fiber tow in axial and transverse direction, respectively.

Obtaining the thermal resistance of each element started with selecting the direction of which we want to know the resistance value of composite materials. Fig. 4-2(e,f) represents a scheme showing that thermal conductivity was calculated in fill strand direction (along x-axis) of a woven fabric composite. As described above, each unit cell was divided into elements of same geometry with $dx \times dy \times dz$, and the center points of the elements determine which substance was located in the elements among fill, warp strand and matrix. If the impregnated fill strand was located at arbitrary element like fig. 4-2(f), θ_f and K_{fill} which denoted the inclination of fill strand with respect to x-axis and the thermal conductivity along the axis were obtained by equation (22) and (23). In the same manner, when selected as a center point, warp strand can be described with only transverse directional conductivity due to orthogonality with respect to the fill strand direction. (Equation (24)) In order to get

thermal properties in the direction of warp strand (y-axis), the same procedure would be applied by exchanging the variables of fill and warp strands with each other.

$$\theta_f = \left| \tan^{-1}\left(\frac{d}{dx} H_f(x)\Big|_{x=a_x} \right) \right| = \left| \tan^{-1}\left(-\frac{h_w}{2} \cos\left(\frac{\pi a_x}{L_w} \right) \right) \right| \tag{22}$$

$$K_{fill} = K_{a,i} \cos^2(\theta_f) + K_{t,i} \sin^2(\theta_f) \tag{23}$$

$$K_{warp} = K_{t,i} \tag{24}$$

4.2.1.3. Woven Fabric Composite Electrical Conductivity Modeling

Unlike thermal conductivity which is influenced by the movement of phonons as well as electrons, only electrons contribute to electrical conductive behavior. GF or epoxy resin whose continuity has a significant impact on thermal conductivity does not exercise its influences on electrical conductivity any more. Major conductive materials are CNTs and CF in multiscale and fiber-reinforced composites, respectively. In this paper, two kinds of modeling methods are utilized for electrical conductivity of woven fabric composites. One was rule-of-mixtures (ROM), the other was Mori-Tanaka method (MTM).

In CNT/GF/epoxy composites, CNTs served as major conductive materials whose property was realized by that of matrix part, a mixture of CNTs and epoxy. Both CNT/GF/epoxy and CF/epoxy composites were merely regarded as the combination of two materials, woven fabric and matrix. In the former case, fiber was electrically conductive whereas in the latter, matrix was conductive. Non-conductive parts in these cases did not perform any role in conducting behavior but filled out the rest volume of the entire composite except conductive parts. So, a concept of effective cross-sectional area was introduced. The required variables related to resistance and conductivity were characteristic length and cross-sectional area along the conductive direction. For example, if it is assumed that electrical conductivity in the fill direction is calculated, information of the length and cross-sectional area of the fill and warp strands and matrix makes it possible to calculate it. Effective cross-sectional area was defined by dividing volume fraction of each strand with characteristic length (refer to Equation (26)), and, on the basis of rule of mixture, effective electrical conductivity was obtained by using the effective cross-sectional area. The effective electrical conductivity in fill strand direction is shown in equation (25).

$$\sigma_{eff} = (\sigma_m A_m + \sigma_f A_f + \sigma_w A_w) / A_{total} \tag{25}$$

$$
\begin{aligned}
A_{total} &= (h_f + h_w)L_f \\
A_f &= Vf_f / L_w \\
A_w &= Vf_w / L_f \\
A_m &= A_{total} - A_f - A_w
\end{aligned}
\tag{26}
$$

σ and A mean the electrical conductivity and effective cross-sectional area of the constituents. Subscripts *f*, *w* and *m* are the same as the case of thermal conductivity as mentioned above. A_{total} represents the cross-sectional area of the composite perpendicular to x-axis.

MTM is the same modeling tool that was described in nanocomposites' conductivity modeling. But the tool was a little bit modified in accordance with the change of several assumptions and conditions to establish a relationship between the fiber and matrix. Basically, CNT and fiber show apparent difference in aspect ratio which Eshelby tensor is a function of. Additionally, it's assumed that in the fiber composites filaments of the fill and warp strands are not sinusoidal form and are dispersed perfectly for the simplicity of modeling. Despite the perfect dispersion of filaments, they are not completely in parallel with each other. Otherwise, they cannot form conductive network and behave like an insulating material in case of the through-thickness modeling of composites. In this paper, the deviation of the filaments ranges from 0 to 3.0% which was from an empirical result considering a unit cell geometry.

4.2.2. Experimental

4.2.2.1. Materials

For multiscale composites, CNTs used in this paper were multiwall CNTs (CM-100) produced by Hanwha Chemical, Korea. Plain-woven GF and CF (T300-grade) which served as reinforcing materials were provided by JMC Co., Korea. The polymer matrix was composed of bisphenol-F type epoxy (YDF-170 from Kukdo Chemical Co., Korea) and a curing agent (SH-101A from Sejin E&C, Korea).[40]

4.2.2.2. Sample Fabrication and Experiments

We have manufactured two kinds of composite samples for validation procedure; CNT/GF/epoxy and CF/epoxy composites. The same manufacturing process used in Sung et al.'s paper [*] was employed for five types of the CNT/GF/epoxy multiscale composites where CNT contents in epoxy resin were varied from 0 to 5 wt.% (0, 0.5, 1, 3, 5 wt.%). And four types of CF/epoxy fiber-reinforced composites were made by varying pressure exerted on the samples during curing process (1, 2, 3, 4 MPa). Thirty-two layers of plane woven CF are mixed with resin through pre-impregnation process and are stacked up by hand-layup on a mold. The stacked composite samples were covered with breather

and vacuum bag and then vacuumed for 20min to remove trapped air. After that, the samples were allowed to be cured at 120ºC under high pressure. LFA 447 (Netzsch, Germany) was utilized to measure the thermal conductivity of the composites, while Keithley 2002 multimeter and CMT-SR2000N were used to perform measurement of the electrical conductivity of the in-plane and through-thickness samples, respectively.

4.3. Results and Discussion

4.3.1. Thermal Conductivity

Since there have been lots of computational results of the thermal and electrical conductivities of nanocomposites with experimental data for validation[31,35,58,61,62], results of the woven fabric conductivity modeling are mainly discussed in this section. Thermal conductivity modeling which makes a composite specimen split into finite elements borrowing thermal-electrical analogy is substantially affected by the geometry of the unit cell and elements mentioned in Section 4.2.1.2. The geometry data of the unit cell are represented in Table 4-1. It is true that the continuity of elements and the reliability of a modeling would be guaranteed when the size of all the elements composing a unit cell is minimized. However, since it has some restrictions in time for the calculation and the complexity, each element size should be optimized. Fig. 4-4 shows that thermal conductivity relies on the height-to-width ratio (H/W ratio) of a unit cell with an element size for optimization. The conductivity of the CF/epoxy composites decreases with increasing H/W ratio, for the volume occupied by matrix at edge of the unit cell increases. In the multiscale composites, the matrix' conductivity is dominant over that of the woven fabric so that one can expect that the thermal conductivity result shows incremental tendency. Seeing from Fig. 4-4 (a-c), the conductivity graphs become stabilized without deviating points. That is, the characteristic length of each side of an element must be less than 0.1% of corresponding length of a unit cell to obtain stabilized results.

Table 4-1 Information of the CNT/GF/epoxy and CF/epoxy samples for comparison

		CNT/GF/epoxy					CF/epoxy			
Sample No.		1	2	3	4	5	6	7	8	9
Fabricating condition	(wt. %)	0	0.5	1	3	5				
	(MPa)						1	2	3	4
Fiber volume fraction (%)		48.5	50.5	46.3	33.6	34.5	63.6	66.9	69.2	69.5
h_f, h_w (mm)		0.07					0.078			
L_f, L_w (mm)		1.06					1.59			

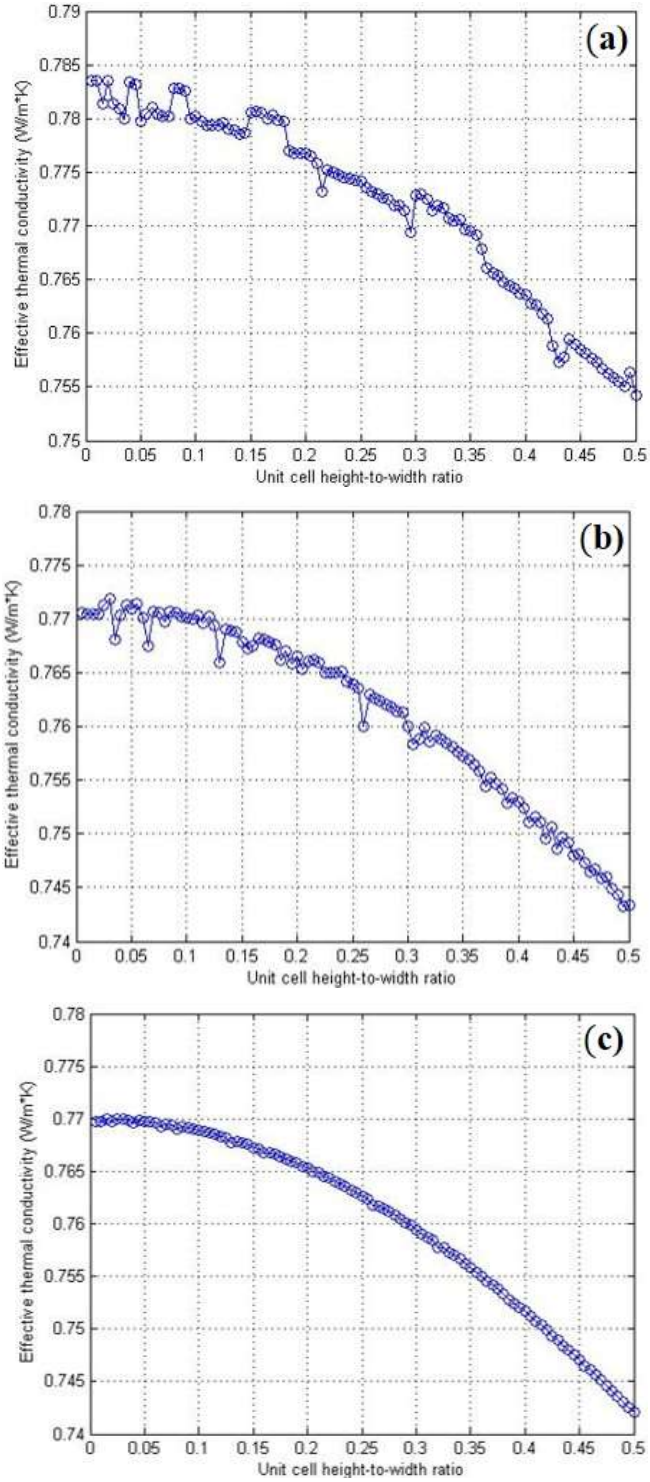

Fig. 4-4 Thermal conductivity vs. Height-to-width ratio of a unit cell with optimizing an element size: (a) $dz = 0.1h$, (b) $dz = 0.01h$, (c) $dz = 0.001h$ (dz and h are the heights of a unit cell and an element)

Predicted modeling results were validated by comparing them with empirical results. As described in Section 2.3, four types of CNT/GF/epoxy composites with various CNT contents (0,1,3,5 wt.%) were produced whereas four CF/epoxy composites were made under different pressures during the curing

process (refer to Table 4-1). It is apparent that the CNTs in Fig. 3-6 are considerably aligned in longitudinal direction of the fiber and the orientation of CNTs are restricted in the range of 70% through SEM image processing. This was from consideration of resin flow in the hand-layup process and in-plane directional woven fabric. Thermal conductivity values of the CNT, GF, and epoxy were, respectively, chosen with 1500 W/m*K[63], 1.2 W/m*K[36] and 0.225 W/m*K from 0.19-0.36 W/m*K[31,36,64] and average aspect ratio of CNTs is 2000 according to product data of CM-100. Fig. 4-5 (a) and (b) represent the in-plane and through-thickness thermal conductivity of the multiscale composites. Most experimental results agree well with simulation results.

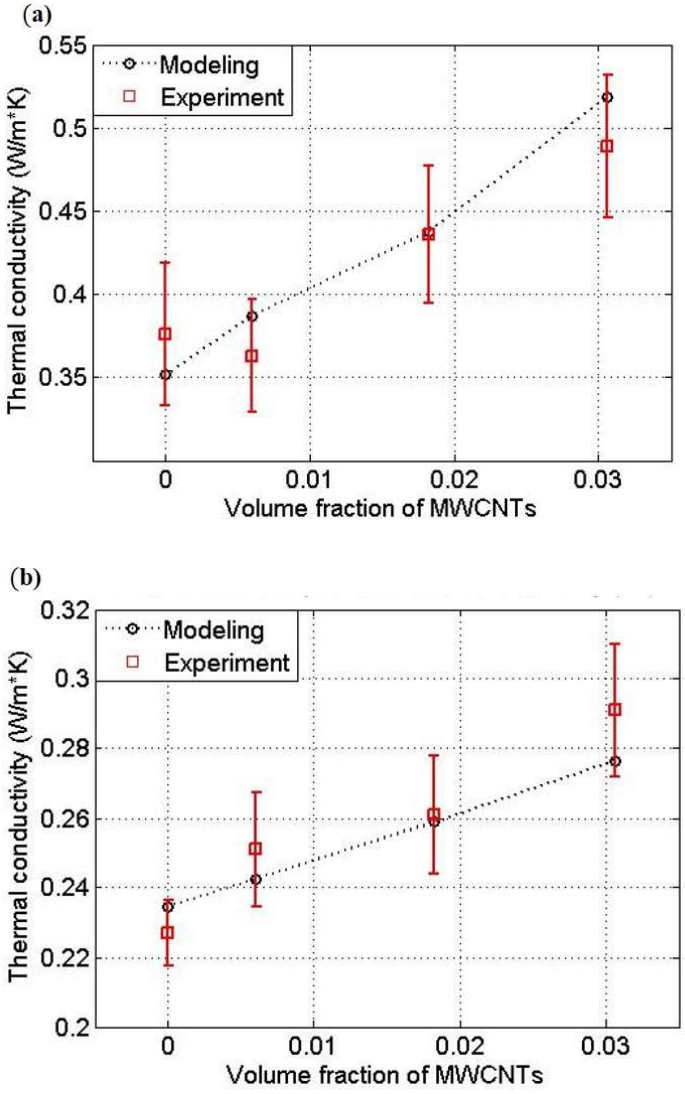

Fig. 4-5 Thermal conductivity modeling and empirical data of CNT/GF/epoxy composites vs. CNT volume fraction: (a) In-plane, (b) Through-thickness

Fig. 4-6 shows thermal conductivities of the fiber-reinforced composites obtained by modeling and measurement. The volume fraction of woven fabric in the composites was from 40 to 80%. Input variables were the thermal conductivity of the two constituents, CF and epoxy, and volume fraction. 22

W/m*K[65] is selected as conductivity of the CF. Comparing two results between in-plane and through-thickness conductivities, we can see that in-plane thermal conductivities are approximately twice as high as through-thickness ones. That is because the continuity of the woven fibers was relatively assured in in-plane direction as compared to the discreteness of the network in through-thickness direction. In the same vein, in-planes result shows linear increment with respect to volume fraction of the CF while through-thickness conductivity has marginally positive parabolic graph. In through-thickness direction, due to the discrete network in both warp and fill strands, the composite manufactured by higher pressure forms more conductive path than that by lower pressure from top to bottom or vice versa. Simulation results were verified by comparing them with those of empirical measurements in both in-plane and through-thickness directions.

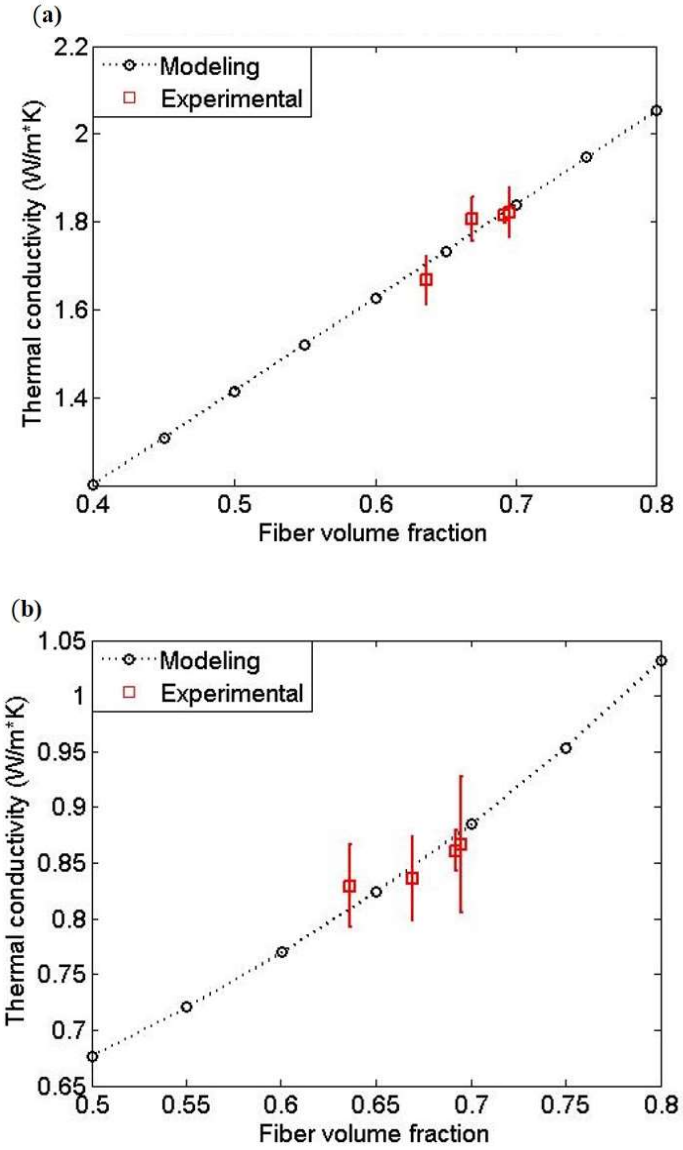

Fig. 4-6 Thermal conductivity modeling and empirical data of CF/epoxy composites vs. CF volume fraction: (a) In-plane, (b) Through-thickness

4.3.2. Electrical Conductivity

Electrical conductivity modeling of the woven fabric composites was implemented by two kinds of methods, rule-of-mixtures (ROM) and Mori-Tanaka method (MTM). Results by the two methods were compared with the experimental results. Fig. 4-7 shows in-plane and through-thickness electrical conductivities of the CF/epoxy composites obtained by the two modeling methods. Diameter of the CF, electrical conductivities of the CF and epoxy as input variables were taken as 8μm, 4.2 S/m and 1E-13 S/m[55], respectively. Fig. 4-8 shows schematic of measurement of electrical conductivity of CF filament in longitudinal direction and the electrical conductivity in transverse direction was calculated using the following relations, Equation (27)-(30).[66]

$$\sigma_t = \frac{d^2\sigma_c\sigma_{\text{int}} + 2\sigma_{\text{int}}(\sigma_c + \sigma_{\text{int}})(t^2 + 2at)}{d^2\sigma_{\text{int}} + 2\sigma_{\text{int}}(\sigma_c + \sigma_{\text{int}})(t^2 + 2at)} \tag{27}$$

$$\sigma_l = \frac{\sigma_c d^2 + \sigma_{\text{int}}(4dt + t^2)}{(d + 2t)^2} \tag{28}$$

$$\sigma_{eff,t} = \frac{2t\sigma_{\text{int}} + \sigma_t l}{l + 2t} \tag{29}$$

$$\sigma_{eff,l} = (l + 2t)\left(\frac{2t}{\sigma_{\text{int}}} + \frac{l}{\sigma_l}\right) \tag{30}$$

where d, a, l and t represent diameter, radius, length of CF and interfacial shell thickness around the CF. Subscripts c, t, l and eff of the electrical conductivity denote intrinsic, transverse, longitudinal conductivity and effective property including consideration of interfacial shell. Unlike CNT of nanoscale filler, however, tunneling effect doesn't account that much for the case of CF but the interfacial conductivity was utilized as a parameter to derive transverse directional conductivity.

Comparing the two methods in fig. 4-7, we can see that slope of MTM is steeper than that of ROM above around 20% of volume fraction. It is because the difference occurred by introducing conductivity concentration tensor on MTM is reflected. No big difference is observed between the two modeling methods for in-plane electrical conductivity in Fig. 4-7(a). For in-plan electrical conductivity of the composites, electrical conductivity of the CF filaments in axial direction is dominant and formation of conducting paths between filaments of CF does not have significant impact. But in the case of the through-thickness conductivity, there is large discrepancy between the results of ROM and MTM. The reason is that ROM considers only the transverse conductivity of CF and the effective cross-sectional area and does not account for fiber's geometry or undulation (orientation), while MTM modeling results can be able to reflect the influence of filaments' orientation. With this reason, MTM is more appropriate

tool for electrical conductivity modeling than ROM. In this paper, the orientation of the CF filaments was inserted to range from 0 to 3.0% which was derived from numerical calculation of the strand's undulation within a unit cell.

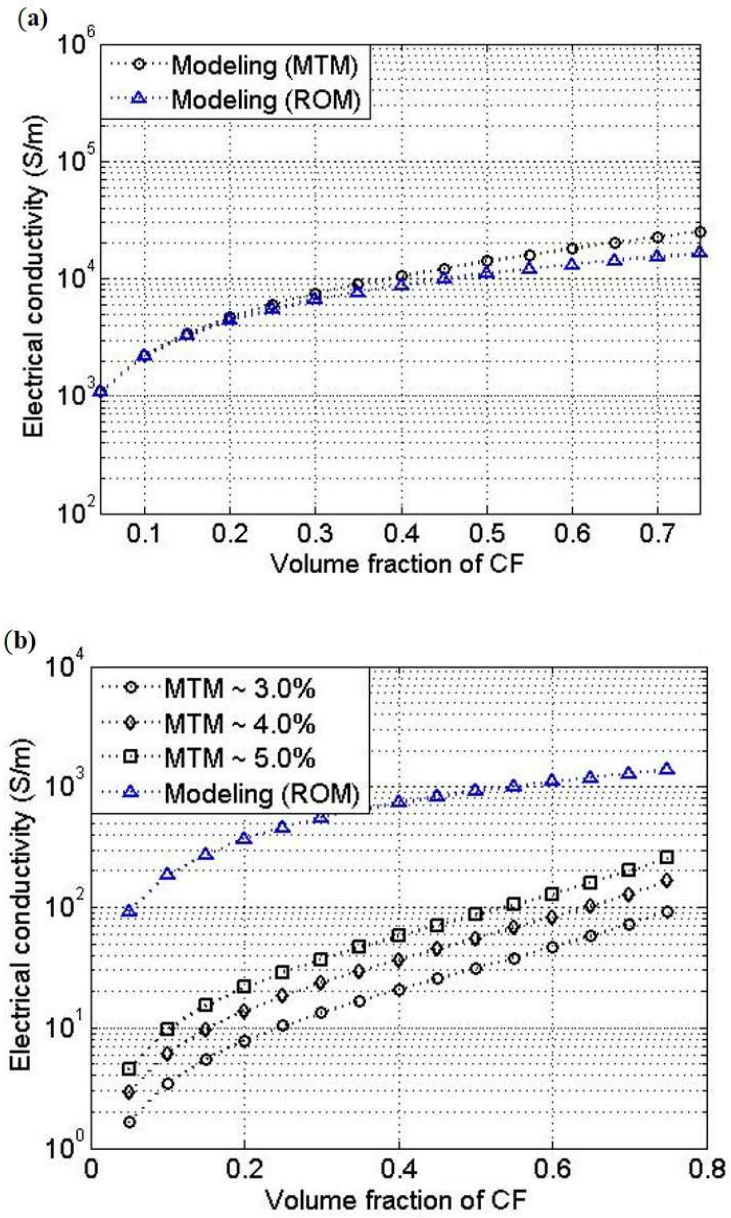

Fig. 4-7 Comparison between Rule of mixture and Mori-Tanaka method: (a) In-plane, (b) Through-thickness

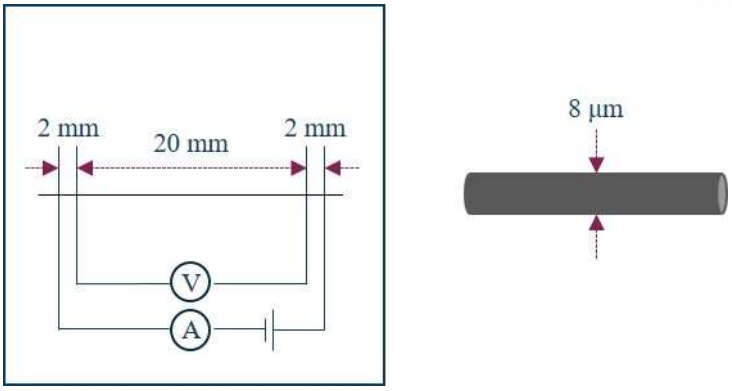

Fig. 4-8 Measurement of electrical conductivity of CF filament

CNT/GF/epoxy multiscale composite is conductive because of CNTs, which induce different conductivity values of the composites by varying their aspect ratio, orientation, volume fraction, etc. Intrinsic electrical conductivity of MWCNT was taken as 3E+4 S/m[67] and the axial and transverse directional conductivity of the CNT were calculated through equations (29) and (30).[66] The electrical conductivity of GF and epoxy and the aligned degree of CNTs were selected as the same values of 1E-13 S/m and 70% which is the number used in thermal conductivity modeling. Fig. 4-9 describes comparison results of experimental and modeling using four types of samples (0.5~5 wt.% of MWCNTs in epoxy). Since electrical conductivity shows percolation behavior unlike thermal conductivity, infinitesimal additional amount of filler makes exponential change in conductive network formation. Though modeling results in both Fig. 4-9 (a) and (b) have relatively similar tendency as compared to experimental results, there is a little gap between them. It's easily explained that the gap is attributed to uncontrollable variables during the empirical process such as the perfect distribution, agglomeration and straightness of CNTs. Results of conductivity modeling and experiments of CF/epoxy fiber-reinforced composites are suggested in Fig. 4-10. As mentioned previously, the input electrical conductivity of CF and epoxy was chosen as 4.2E+4 S/m and 1E-13 S/m, respectively. It's demonstrated that the modeling results are well matched with those of experiments for both in-plane and through-thickness conductivity. Predictability for fiber-reinforced composites is comparatively more desirable than that for multiscale composites in that the conducting constituent of the CF/epoxy composites is easy to handle in manufacturing process and has less variables than the CNT of the CNT/GF/epoxy composites.

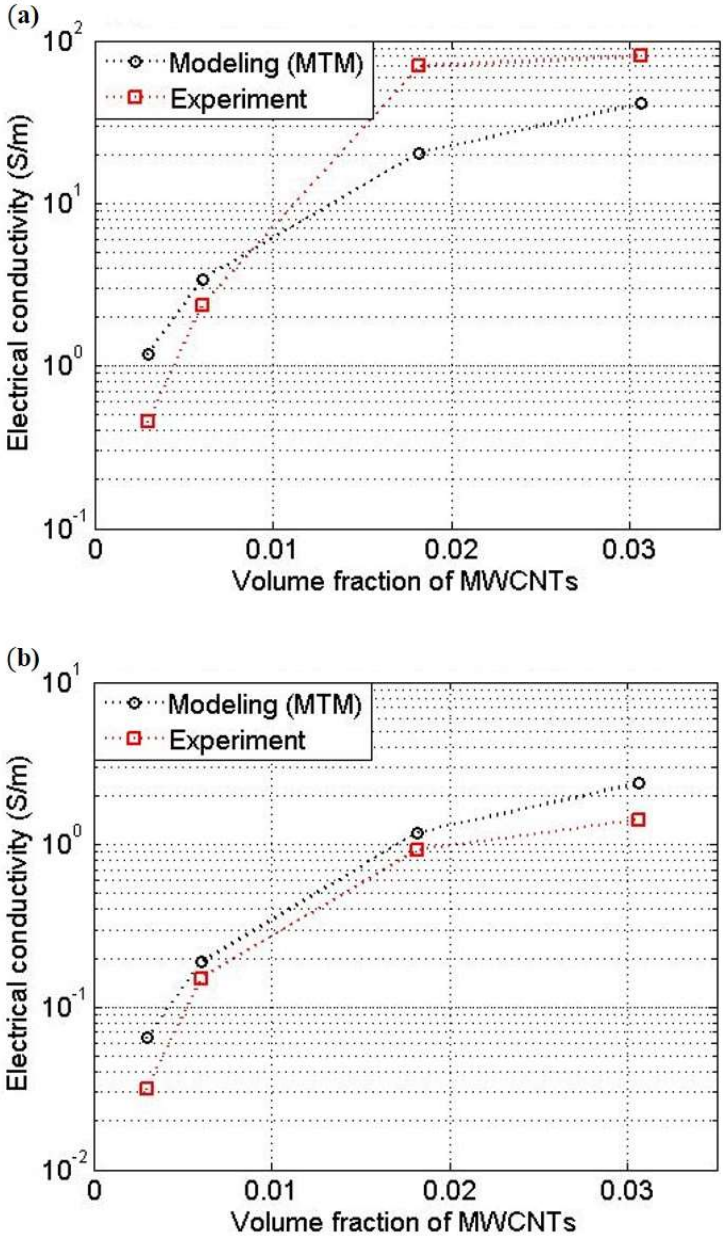

Fig. 4-9 Electrical conductivity modeling and empirical data of CNT/GF/epoxy composites vs. CNT volume fraction: (a) In-plane, (b) Through-thickness

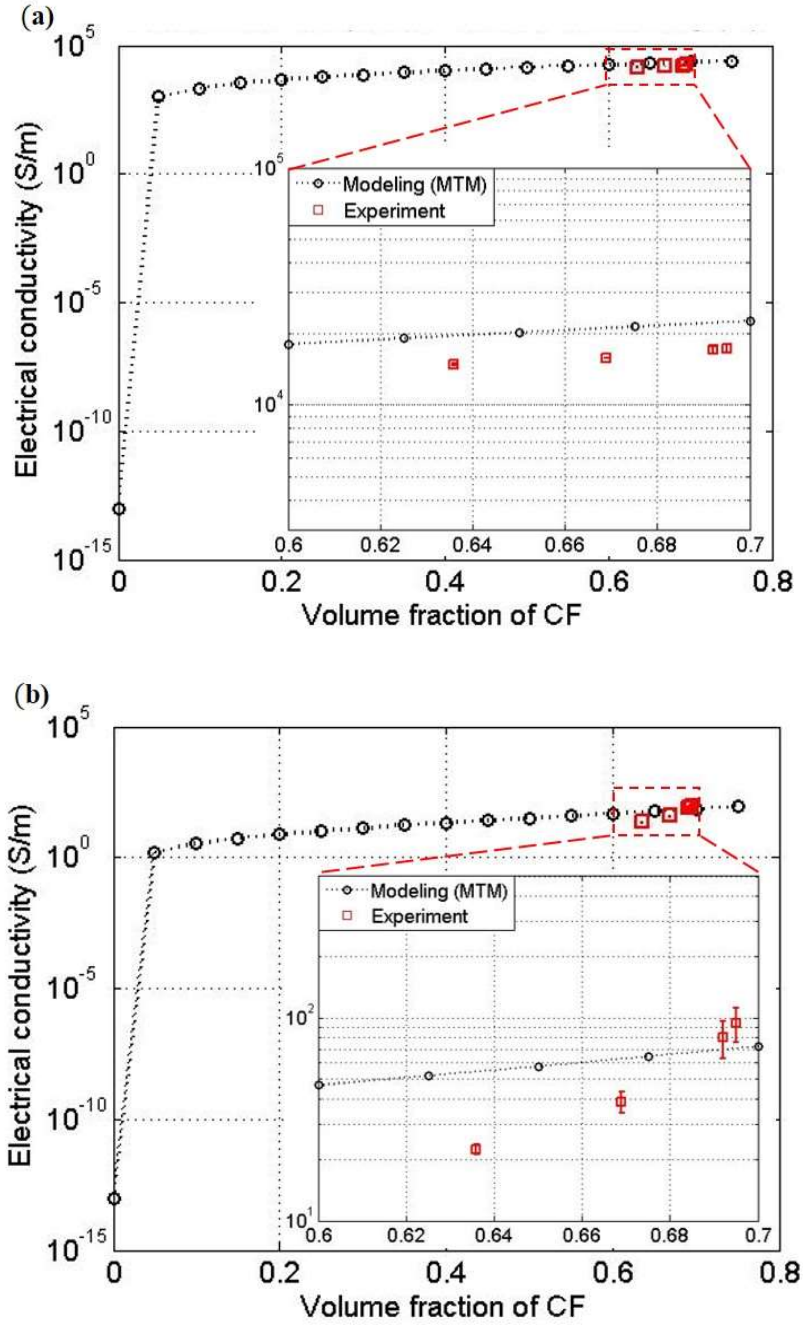

Fig. 4-10 Electrical conductivity modeling and empirical data of CF/epoxy composites vs. CF volume fraction: (a) In-plane, (b) Through-thickness

4.4. Summary

In this chapter, modeling approaches combining the methods for nanocomposites and woven fabric composites were proposed to predict thermal and electrical conductivity of multiscale and fiber-reinforced composites. We have primarily focused on the model of woven fabric composites dealing with the relationship between the constituting woven fabric and matrix. Thermal-electrical analogy and modified Mori-Tanaka method were employed to derive the effective thermal and electrical

conductivities of woven fabric composites, respectively. Both approaches took fiber volume fraction, conductivity, aspect ratio, continuity and undulation into account. Thermal conductivity modeling was stabilized by optimizing the element size of a unit cell which consists of finite elements. In the model for electrical conductivity, it was concluded that Mori-Tanaka method had superiority over rule-of-mixtures which merely considered the effective cross-sectional areas and characteristic lengths of composites. CNT/GF/epoxy composites and CF/epoxy composites were manufactured to compare their conductivity values with those of the modeling. Comparison indicated that modeling results well agreed with empirical data and have close tendency with respect to the manufacturing variables.

5. Conclusions

5.1. Conclusions

Multifunctionality of structural composites, especially laminated fabric composites, has been expanded to diverse fields such as self-sensing, self-healing, actuating, and electromagnetic interference shielding. It has been found out that the study of woven fiber composites as thermoelectric materials will render the versatile composites useful and profitable since structural components are likely to be exposed to temperature gradient or redundant heat flow in service.

In Chapter 3, thermoelectric properties and potential for thermal energy harvesting of CNT/GF/epoxy multiscale composites and CF/epoxy fiber-reinforced composites were mainly studied. The test samples were manufactured by pre-impregnated process and hand lay-up technique. We conducted measurements of three significant variables, namely, Seebeck coefficient, electrical conductivity and thermal conductivity, which constitute figure of merit, the thermoelectric efficiency. Seebeck coefficients indicated that multiscale and fiber-reinforced composites exhibited n- and p-type semiconducting material behaviors, respectively. For thermal or electrical conductivity, inclusion of CNT which served as dominant conducting material enhanced the conductivities. Alignment of CNTs along the GF in multiscale composites and continuity of CF in fiber composites had a significant impact on the improvement of in-plane conductivity as compared to through-thickness conductivity. Maximum figure of merit calculated from above variables was ~10E-5, which is far below the standard for commercialization. However, the potential of the composites as thermoelectric materials has been confirmed via demonstration of electrical current generation from a closed circuit of two different types of materials.

Chapter 4 demonstrated conductivity model approaches of the composites made up of CNT, GF, CF, and epoxy. In the multiscale composite model, the point was combining the nanocomposite model and woven fabric composite model by replacing the property of matrix of fabric composite with the resultant conductivity of nanocomposite. We made up for the weak points of existing uses of thermal-electrical analogy method in predicting thermal conductivity of woven fiber composites by introducing infinitesimal elements which had their own thermal resistance. As for electrical conductivity, a comparison between rule-of-mixtures and modified Mori-Tanaka method was made in terms of capability to take into account various aspects of the composites. The Mori-Tanaka method exhibited better performance with regard to simplicity and consideration of flexibility. These approaches were successfully validated via measuring their results against the empirical data obtained by varying CNT concentrations or CF volume fraction.

5.2. Recommendations for Future Work

One of the most important remaining tasks is enhancement of thermoelectric efficiency for the sake of commercialization in the moderate temperature range. Figure of merit (ZT) of composite materials should become one digit or more values to make use of ambient temperature economically. Fundamental understanding of Seebeck coefficient and its numerical model will make it possible to optimize figure of merit with established modeling approaches of thermal and electrical conductivity in this study.

References

1. Andres, R. J.; Gregg, J. S.; Losey, L.; Marland, G.; Boden, T. A., Monthly, global emissions of carbon dioxide from fossil fuel consumption. *Tellus B* **2011,** *63* (3), 309-327.

2. Xi, H.; Luo, L.; Fraisse, G., Development and applications of solar-based thermoelectric technologies. *Renewable and Sustainable Energy Reviews* **2007,** *11* (5), 923-936.

3. Park, Y.; Yoon, C.; Lee, C.; Shirakawa, H.; Suezaki, Y.; Akagi, K., Conductivity and thermoelectric power of the newly processed polyacetylene. *Synthetic Metals* **1989,** *28* (3), D27-D34.

4. Zuzok, R.; Kaiser, A.; Pukacki, W.; Roth, S., Thermoelectric power and conductivity of iodine-doped "new"polyacetylene. *The Journal of chemical physics* **1991,** *95* (2), 1270-1275.

5. Maddison, D.; Unsworth, J.; Roberts, R., Electrical conductivity and thermoelectric power of polypyrrole with different doping levels. *Synthetic metals* **1988,** *26* (1), 99-108.

6. Yan, H.; Sada, N.; Toshima, N., Thermal transporting properties of electrically conductive polyaniline films as organic thermoelectric materials. *Journal of Thermal Analysis and Calorimetry* **2002,** *69* (3), 881-887.

7. Yao, Q.; Chen, L.; Zhang, W.; Liufu, S.; Chen, X., Enhanced thermoelectric performance of single-walled carbon nanotubes/polyaniline hybrid nanocomposites. *Acs Nano* **2010,** *4* (4), 2445-2451.

8. McGrail, B. T.; Sehirlioglu, A.; Pentzer, E., Polymer composites for thermoelectric applications. *Angewandte Chemie International Edition* **2015,** *54* (6), 1710-1723.

9. Li, X.; Maute, K.; Dunn, M. L.; Yang, R., Strain effects on the thermal conductivity of nanostructures. *Physical Review B* **2010,** *81* (24), 245318.

10. Nielsch, K.; Bachmann, J.; Kimling, J.; Böttner, H., Thermoelectric nanostructures: from physical model systems towards nanograined composites. *Advanced Energy Materials* **2011,** *1* (5), 713-731.

11. Dynys, F.; Sayir, A.; Mackey, J.; Sehirlioglu, A., Thermoelectric properties of WSi 2–SixGe 1− x composites. *Journal of Alloys and Compounds* **2014,** *604*, 196-203.

12. Kamarudin, M. A.; Sahamir, S. R.; Datta, R. S.; Long, B. D.; Mohd Sabri, M. F.; Mohd Said, S., A review on the fabrication of polymer-based thermoelectric materials and fabrication methods. *The Scientific World Journal* **2013,** *2013*.

13. Zhang, B.; Sun, J.; Katz, H.; Fang, F.; Opila, R., Promising thermoelectric properties of commercial PEDOT: PSS materials and their Bi2Te3 powder composites. *ACS applied materials & interfaces* **2010,** *2* (11), 3170-3178.

14. Zhao, L.; Sun, X.; Lei, Z.; Zhao, J.; Wu, J.; Li, Q.; Zhang, A., Thermoelectric behavior of aerogels based on graphene and multi-walled carbon nanotube nanocomposites. *Composites Part B: Engineering* **2015,** *83*, 317-322.

15. Meng, C.; Liu, C.; Fan, S., A promising approach to enhanced thermoelectric properties using carbon nanotube networks. *Advanced materials* **2010,** *22* (4), 535-539.

16. Yu, C.; Kim, Y. S.; Kim, D.; Grunlan, J. C., Thermoelectric behavior of segregated-network polymer nanocomposites. *Nano letters* **2008,** *8* (12), 4428-4432.

17. Hewitt, C. A.; Kaiser, A. B.; Roth, S.; Craps, M.; Czerw, R.; Carroll, D. L., Multilayered carbon nanotube/polymer composite based thermoelectric fabrics. *Nano letters* **2012,** *12* (3), 1307-1310.

18. Moriarty, G. P.; De, S.; King, P. J.; Khan, U.; Via, M.; King, J. A.; Coleman, J. N.; Grunlan, J. C., Thermoelectric behavior of organic thin film nanocomposites. *Journal of Polymer Science Part B: Polymer Physics* **2013,** *51* (2), 119-123.

19. Mallick, P. K., *Fiber-reinforced composites: materials, manufacturing, and design*. CRC press: 2007.

20. Gibson, R. F., A review of recent research on mechanics of multifunctional composite materials and structures. *Composite structures* **2010,** *92* (12), 2793-2810.

21. Vlasveld, D.; Bersee, H.; Picken, S., Nanocomposite matrix for increased fibre composite strength. *Polymer* **2005,** *46* (23), 10269-10278.

22. Zhao, Z.-G.; Ci, L.-J.; Cheng, H.-M.; Bai, J.-B., The growth of multi-walled carbon nanotubes with different morphologies on carbon fibers. *Carbon* **2005,** *43* (3), 663-665.

23. Todoroki, A.; Tanaka, M.; Shimamura, Y., Electrical resistance change method for monitoring delaminations of CFRP laminates: effect of spacing between electrodes. *Composites Science and Technology* **2005,** *65* (1), 37-46.

24. Todoroki, A.; Omagari, K.; Shimamura, Y.; Kobayashi, H., Matrix crack detection of CFRP using electrical resistance change with integrated surface probes. *Composites science and technology* **2006,** *66* (11), 1539-1545.

25. Sebastian, J.; Schehl, N.; Bouchard, M.; Boehle, M.; Li, L.; Lagounov, A.; Lafdi, K., Health monitoring of structural composites with embedded carbon nanotube coated glass fiber sensors. *Carbon* **2014,** *66*, 191-200.

26. Blaiszik, B.; Kramer, S.; Olugebefola, S.; Moore, J. S.; Sottos, N. R.; White, S. R., Self-healing polymers and composites. *Annual Review of Materials Research* **2010,** *40*, 179-211.

27. Patrick, J. F.; Hart, K. R.; Krull, B. P.; Diesendruck, C. E.; Moore, J. S.; White, S. R.; Sottos, N. R., Continuous Self-Healing Life Cycle in Vascularized Structural Composites. *Advanced Materials* **2014,** *26* (25), 4302-4308.

28. Hiroshi, H.; Minoru, T., Equivalent inclusion method for steady state heat conduction in composites. *International Journal of Engineering Science* **1986,** *24* (7), 1159-1172.

29. Hatta, H.; Taya, M., Effective thermal conductivity of a misoriented short fiber composite. *Journal of Applied Physics* **1985,** *58* (7), 2478-2486.

30. Chen, C.-H.; Wang, Y.-C., Effective thermal conductivity of misoriented short-fiber reinforced thermoplastics. *Mechanics of Materials* **1996,** *23* (3), 217-228.

31. Yu, J.; Lacy, T. E.; Toghiani, H.; Pittman, C. U., Micromechanically-based effective thermal conductivity estimates for polymer nanocomposites. *Composites Part B: Engineering* **2013,** *53*, 267-273.

32. Yan, K.; Xue, Q.; Zheng, Q.; Hao, L., The interface effect of the effective electrical conductivity of carbon nanotube composites. *Nanotechnology* **2007,** *18* (25), 255705.

33. Deng, F.; Zheng, Q.-S., An analytical model of effective electrical conductivity of carbon nanotube composites. *Applied Physics Letters* **2008,** *92* (7), 071902.

34. Li, C.; Thostenson, E. T.; Chou, T.-W., Effect of nanotube waviness on the electrical conductivity of carbon nanotube-based composites. *Composites Science and Technology* **2008,** *68* (6), 1445-1452.

35. Dalmas, F.; Dendievel, R.; Chazeau, L.; Cavaillé, J.-Y.; Gauthier, C., Carbon nanotube-filled polymer composites. Numerical simulation of electrical conductivity in three-dimensional entangled fibrous networks. *Acta Materialia* **2006,** *54* (11), 2923-2931.

36. Ning, Q.-G.; Chou, T.-W., Closed-form solutions of the in-plane effective thermal conductivities of woven-fabric composites. *Composites science and technology* **1995,** *55* (1), 41-48.

37. Ning, Q.-G.; Chou, T.-W., A closed-form solution of the transverse effective thermal conductivity of woven fabric composites. *Journal of Composite Materials* **1995,** *29* (17), 2280-2294.

38. Dasgupta, A.; Agarwal, R.; Bhandarkar, S., Three-dimensional modeling of woven-fabric composites for effective thermo-mechanical and thermal properties. *Composites science and technology* **1996,** *56* (3), 209-223.

39. Seo, B. H.; Cho, Y. J.; Youn, J. R.; Chung, K.; Kang, T. J.; Park, J. K., Model for thermal conductivities in spun yarn carbon fabric composites. *Polymer composites* **2005,** *26* (6), 791-798.

40. Sung, D. H.; Kang, G.-H.; Kong, K.; Kim, M.; Park, H. W.; Park, Y.-B., Characterization of thermoelectric properties of multifunctional multiscale composites and fiber-reinforced composites for thermal energy harvesting. *Composites Part B: Engineering* **2016,** *92*, 202-209.

41. Rowe, D. M., *Thermoelectrics handbook: macro to nano*. CRC press: 2005.

42. Hillhouse, H. W.; Tuominen, M. T., Modeling the thermoelectric transport properties of nanowires embedded in oriented microporous and mesoporous films. *Microporous and Mesoporous Materials* **2001,** *47* (1), 39-50.

43. Barbero, E. J., *Introduction to composite materials design*. CRC press: 2010.

44. Wang, S.; Qiu, J., Enhancing thermal conductivity of glass fiber/polymer composites through carbon nanotubes incorporation. *Composites Part B: Engineering* **2010,** *41* (7), 533-536.

45. Kanari, K.; Ozawa, T., Thermal Conductivity of Epoxy Resins Cured with Aliphatic Amines. *Polym J* **1973,** *4* (4), 372-378.

46. Zhong, C.; Yang, Q.; Wang, W., Correlation and prediction of the thermal conductivity of amorphous polymers. *Fluid Phase Equilibria* **2001,** *181* (1–2), 195-202.

47. Aliev, A. E.; Lima, M. H.; Silverman, E. M.; Baughman, R. H., Thermal conductivity of multi-walled carbon nanotube sheets: radiation losses and quenching of phonon modes. *Nanotechnology* **2010,** *21* (3), 035709.

48. Levinson, R.; Akbari, H.; Gartland, L., *Impact of the temperature dependency of fiberglass insulation R-value on cooling energy use in buildings*. 1996; p Medium: ED; Size: 13 p.

49. Hartwig, G.; Knaak, S., Fibre-epoxy composites at low temperatures. *Cryogenics* **1984,** *24* (11), 639-647.

50. Lin, W.; Moon, K.-S.; Wong, C. P., A Combined Process of In Situ Functionalization and Microwave Treatment to Achieve Ultrasmall Thermal Expansion of Aligned Carbon Nanotube-Polymer Nanocomposites: Toward Applications as Thermal Interface Materials. *Advanced Materials* **2009,** *21* (23), 2421-2424.

51. Park, J.; Cheng, Q.; Lu, J.; Bao, J.; Tian, Y.; Liang, R.; Wang, B.; Zhang, C.; Brooks, J. S. In *High thermal conductivity of carbon nanotube sheet/epoxy composite*, 18th International conference on composite materials, 2011.

52. Wan, M.; Yadav, R. R.; Singh, D.; Sridhar Panday, M.; Rajendran, V., Temperature dependent ultrasonic and thermo-physical properties of polyaniline nanofibers reinforced epoxy composites. *Composites Part B: Engineering* **2016,** *87*, 40-46.

53. Fujita, S.; Suzuki, A., *Quantum Theory of Thermoelectric Power (Seebeck Coefficient)*. 2011.

54. Tritt, T. M., Thermoelectric phenomena, materials, and applications. *Annual review of materials research* **2011,** *41*, 433-448.

55. Feng, C.; Jiang, L., Micromechanics modeling of the electrical conductivity of carbon nanotube (CNT)–polymer nanocomposites. *Composites Part A: Applied Science and Manufacturing* **2013,** *47*, 143-149.

56. Scida, D.; Aboura, Z.; Benzeggagh, M. L.; Bocherens, E., Prediction of the elastic behaviour of hybrid and non-hybrid woven composites. *Composites Science and Technology* **1998,** *57* (12), 1727-1740.

57. Taya, M., *Electronic composites: modeling, characterization, processing, and MEMS applications*. Cambridge University Press: 2005.

58. Seidel, G. D.; Lagoudas, D. C., A micromechanics model for the electrical conductivity of nanotube-polymer nanocomposites. *Journal of Composite Materials* **2009,** *43* (9), 917-941.

59. Liu, G. R., A step-by-step method of rule-of-mixture of fiber- and particle-reinforced composite materials. *Composite Structures* **1997,** *40* (3-4), 313-322.

60. CLAYTON, W., Constituent and composite thermal conductivities of phenolic-carbon and phenolic- graphite ablators(Thermal conductivity prediction during ablation of phenolic-carbon and phenolic-graphic composites for heating and cooling conditions). **1971**.

61. Bao, W. S.; Meguid, S. A.; Zhu, Z. H.; Meguid, M. J., Modeling electrical conductivities of nanocomposites with aligned carbon nanotubes. *Nanotechnology* **2011,** *22* (48), 485704.

62. Bao, W. S.; Meguid, S. A.; Zhu, Z. H.; Weng, G. J., Tunneling resistance and its effect on the electrical conductivity of carbon nanotube nanocomposites. *Journal of Applied Physics* **2012,** *111* (9), 093726.

63. Kim, P.; Shi, L.; Majumdar, A.; McEuen, P. L., Mesoscopic thermal transport and energy dissipation in carbon nanotubes. *Physica B: Condensed Matter* **2002,** *323* (1–4), 67-70.

64. Mohapatra, R. C.; Mishra, A.; Choudhury, B. B., Measurement on Thermal Conductivity of Pine Wood Dust Filled Epoxy Composites. *American Journal of Mechanical Engineering* **2014,** *2* (4), 114-119.

65. Hinoki, T.; Kohyama, A. In *Tensile and Thermal Properties of Chemically Vapor-infiltrated Silicon Carbide Composites of Varous High-modulus Fiber Reinforcements*, Mechanical Properties and Performance of Engineering Ceramics and Composites: A Collection of Papers Presented at the 29th International Conference on Advanced Ceramics and Composites, Jan 23-28, 2005, Cocoa Beach, FL, Ceramic Engineering and Science Proceedings, Vol 26, John Wiley & Sons: 2009; p 311.

66. Pal, G.; Kumar, S., Multiscale modeling of effective electrical conductivity of short carbon fiber-carbon nanotube-polymer matrix hybrid composites. *Materials & Design* **2016,** *89*, 129-136.

67. Ebbesen, T.; Lezec, H.; Hiura, H.; Bennett, J.; Ghaemi, H.; Thio, T., Electrical-conductivity of individual carbon nanotubes. *Nature* **1996,** *382* (6586), 54-56.

Acknowledgements

It would never have been possible to complete this master's thesis without the help, guidance and support of many people.

First and foremost, I would like to express profound gratitude and special thanks to my advisor, Professor Young-Bin Park. He offered me a precious chance to join his lab, and it was a great pleasure to be a member of FIM Lab. Without his unbounded confidence, incredible patience and timely wisdom, my work would have been an overwhelming pursuit. His counsel and advice on both research and my career have been priceless. I would also like to show my deep appreciation to Professor Myungsoo Kim for his heartfelt guidance. He has been liberal with his advice not only on study but also on mental aspect. Additionally, I would like to thank my committee members, Professor Hyung Wook Park, Professor Han Gi Chae, and Professor Wooseok Ji for serving as my committee members despite their busy schedule. They let me have my defense an enjoyable time, and their insightful comments and suggestions improved my thesis quality. Many thanks to our lab members, Dr. Biplab K. Deka, Dr. Ankita Hazarika, Dr. Sang-Ha Hwang for their helpful advice and Byeong-Joo Kim, Gu-Hyeok Kang, Beom Gon Cho, Changyoon Jeong, Hyung Doh Roh, Homin Lee, Chan Woo Jeong, In-Yong Lee for their cooperation and commitment. I could spend pleasant time in the lab thanks to them.

I am grateful to my family members, my parents and younger brother. They always support and encourage me both materially and spiritually. And I would like to thank all of my soccer club members who have spent most of the college life with me and made my school life an joyful moment since undergraduate course. May joy and peace abide in us all.